

**Effect of Water Depth on the Behaviour of Triangular Tension Leg Platform (TLP)**

by

MOHD AZIM BIN MOHD KHALID

Dissertation submitted in partial fulfillment of  
the requirements for the  
Bachelor of Engineering (Hons)  
(Civil Engineering)

JULY 2008

Universiti Teknologi PETRONAS  
Bandar Seri Iskandar  
31750 Tronoh  
Perak Darul Ridzuan

CERTIFICATION OF APPROVAL

**Effect of Water Depth on the Behaviour of Triangular Tension Leg Platform (TLP)**

by

Mohd Azim bin Mohd Khalid

A project dissertation submitted to the  
Civil Engineering Programme  
University Technology of PETRONAS  
In partial fulfillment of the requirement for the  
Bachelor of Engineering (Hons)  
(Civil Engineering)

Approved by,



Dr Kurian V. John  
Associate Professor  
Civil Engineering Department  
Universiti Teknologi PETRONAS  
Bandar Seri Iskandar, 31750 Tronoh  
Perak Darul Ridzuan, MALAYSIA

(AP DR. KURIAN V. JOHN)

Co. Supervisor: MR. KALAIKUMAR A/L VALLYUTHAM

UNIVERSITY TECHNOLOGY OF PETRONAS

TRONOH, PERAK

July 2008

## **ACKNOWLEDGEMENT**

First and foremost, pray to God the Al-Mighty for His bless and love, giving me all the strength to complete the final year research project. After everything had been planned, efforts were made, the project managed to be finished within the time frame. Without the help and guidance from other people, this study would not be able to complete successfully. Hence, on this page I would like to express my gratitude to those parties who had directly or indirectly involved helping me in this project.

I would to dedicate this project as a token of gift to my beloved parents, Mohd Khalid bin Mohamed and Siti Radizah binti Abd Samad for their never ending support and pray. Not to forget to both of my lovely sisters, Shariza and Sharina who had been very encouraging and always remind me whenever I forget.

My truly deepest appreciation goes to AP Dr. Kurian V. John, for his expertise, knowledge, ideas and thoughts. Without his guidance, the project would not been able to accomplish accordingly. I would also like to thank Mr. Kalaikumar Vallyutham as my supervisor who had been very supportive and hoping for the very best of the outcome of the research. His advices were of valuable and priceless.

Last but not least, thanks very much to my fellow colleagues, Rasydan, and Azimah, for helping a lot in the finding and analyzing of the research project. Those precious moments spending time together discussing and sharing information will always be remembered.

Again, thank you very much.

# TABLE OF CONTENTS

<b>CERTIFICATE</b> .....	<b>ii</b>
<b>ABSTRACT</b> .....	<b>iv</b>
<b>ACKNOWLEDGEMENT</b> .....	<b>v</b>
<b>CHAPTER 1</b> .....	<b>1</b>
<b>INTRODUCTION</b> .....	<b>1</b>
Background of Study .....	1
1.2 Problem Statement.....	3
1.3 Objectives .....	6
1.4 Scope of Study.....	6
<b>CHAPTER 2</b> .....	<b>8</b>
LITERATURE REVIEW.....	8
<b>CHAPTER 3</b> .....	<b>16</b>
METHODOLOGY .....	16
3.1 Research.....	17
3.2 Conduct Analysis.....	18
3.3 Software required.....	18
3.4 Health, Safety & Environment (HSE) Analysis .....	20
<b>CHAPTER 4</b> .....	<b>21</b>
RESULTS AND DISCUSSIONS .....	21
4.1 Dimensional and Environmental Data.....	21
4.2 Coordinate system of triangular TLP.....	22
4.3 Analysis on Wave Spectrum .....	22
4.4 Analysis of Wave Time Series.....	24
4.5 Analysis on surge response.....	27
4.51 Parameters in surge analysis .....	27

# ***CHAPTER 1***

## ***INTRODUCTION***

### **Background of Study**

An offshore structure can be defined as one which has no fixed access to dry land. It is required to stay in position in all weather conditions. The offshore structure should experience small motion to provide stable working condition for operations such as drilling and production of oil. Fixed structures experience greater forces than compliant structures in viable environment such as an ocean. [1]

Many types of structural systems have been proposed to enhance the water depth capability of offshore structures. The tension-leg platform (TLP) is one of the promising concepts. A TLP is a floating structure, vertically moored to the seabed by a system of pre-tensioned tethers held in tension by the buoyancy of the hull. This approach restrains vertical motions (heave, pitch, and roll) but allows horizontal movements (surge, sway, and yaw). A typical compliant offshore platform is exposed to a combination of environmental loads such as winds, waves and currents. [2]

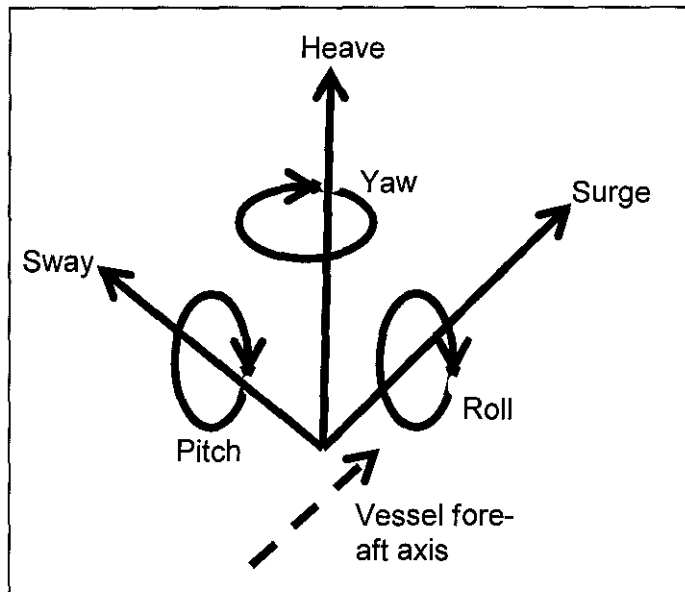


Figure 1.0: Six degree of freedom

Study aims to investigate the effects of water depth on responses (surge, heave, and pitch) of triangular TLP, as shown in Figure 1.0. In the research, wave theories are applied for calculating waves and forces acting on the structure. Researches were conducted involving finding the historical events of TLPs installation in the world, the functions, global water depth significant changes, and TLP dimensional platform and environmental data.

A parametric study will be conducted to analyze the effects of water depth on the responses of a triangular TLP. The dimensions of platform and environmental data are to be assumed at certain values, and the water depth value is varying. As for the study, Brutus TLP was chosen and few alterations were made since there had never been a triangular TLP ever constructed in the ocean of the world.

## 1.2 Problem Statement

A typical compliant offshore platform is exposed to a combination of environmental loads such as winds, waves and currents. There are two non-linear aspects that have to be taken into account when designing TLP, one relates to the amount of offset (min value of horizontal response) and another one is the limit (minimum or maximum values) of tendon tension forces. As far as the functions of a TLP is concerned, floatation is one the most crucial components. Therefore, water depth incorporates significantly when it comes to designing TLP. A triangular shape TLP is chosen because as far as the TLP design is concerned, three columns structure is less stable. In the history of the tension leg platform, triangular shape structure has been proposed, but yet not built. [2]

Oil exploration and production (E&P) companies are drilling further out into the sea, deeper under the ocean floor (more than 1000 feet) to tap into the pockets of oil and natural gas. [3]

Although, deepwater was once prohibitively expensive, high oil prices make the economics of deepwater drilling economically feasible. Factors affecting this E&P frontier include:

- Strong worldwide demand for energy, especially from burgeoning economies like China bolster the increasing price for oil and, to a lesser extent, natural gas
- Traditional oil producing basins have matured, particularly on land, and exploration & production companies have started to look for new reserves in challenging, deepwater environments in the deepwater Gulf of Mexico. [3]

Apart from that, the need to get into more deepwater oil exploration, another factor which contributes to the idea of the study is the greenhouse warming. Green house warming is a

mechanism preventing radiation from being transferred out of Earth's atmosphere. This condition is due to gaseous substances like carbon dioxide, carbon monoxide that absorb radiation from the sun light and other heat sources and keeping them from being radiated. The repercussion is the increasing global temperature subjected to high amount of heat capacity trapped. [4]

The phenomenon occurs due to many events conducted by both natural and human activities. Natural activities such as volcanic eruption, respiration, organic decay and weathering of calcareous rocks release carbon dioxide. Human activities like burning fuel, deforestation, industrialization, and land-use changes have caused a significant increment of carbon dioxide. [4]

Models of earth climate named General Circulation Models suggesting that the doubling of carbon dioxide will lead to an increase in global temperature of 1.4°C to 4.5°C in the 21<sup>st</sup> century. Models added that decreasing of oceans water level only happen during the glacial period thousands years ago where sea level drop from 80m to 120m due to the growth of glaciers. [5]

Greenhouse effects will lead to increasing water depth of the oceans of the world. As seawater warms, its volume expands. Meanwhile, freshwater which is stored in polar continental regions melts and flows as input to sea, thus contributes to sea-level rise. In the last 100 years, tide-gauge records show a general increase in sea-level of  $2.4 \pm 0.9$  mm per year (Peltier and Tushingham 1989). About 70% of increasing water depth results from thermal expansion of ocean and 30% from melting glaciers that flows freshwater into the sea. [4]

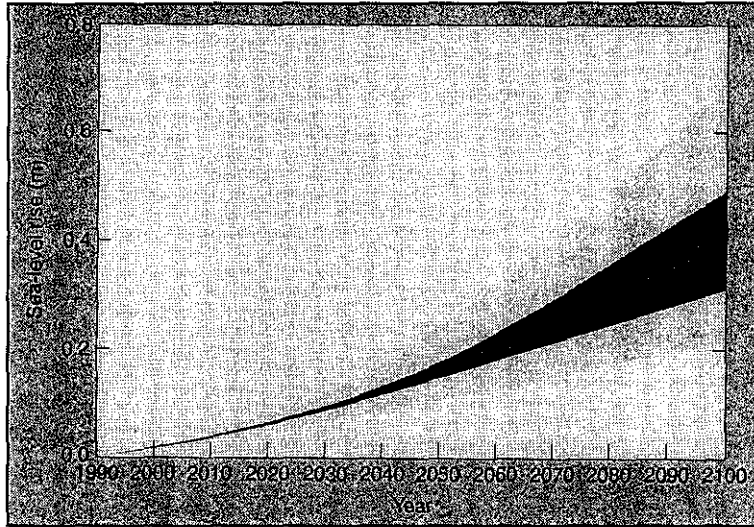


Figure 1.1: Global average sea-level rises from 1990 to 2100. [4]

Figure 1.1 presents the global average sea-level rise from 1990 to 2100. The region on dark shading is the average of seven climate models. Oil and gas industries of the world had embarked about going into ultra deepwater exploration and more hostile environments due to shortage of oil reservoirs in land and shoreline. Development in deepwater production has progressed most rapidly in the Gulf of Mexico. The latest record breaking unit is the Noble Clyde Boudreaux (Silvertip), a semi-submersible production unit in 2,900m (9,356 ft) water depth, which operated by Shell Offshore Inc. Moreover, global warming factor also applies slightly to the increasing water depth, but surely. [3]

As a whole, study focuses on the effect of water depth on the behaviours of TLP to found out the possibilities that a designed TLP for certain water depth can suits in other different water depth as well, as far as water depth is the only parameter concerned.

### **1.3 Objectives**

- To prepare detailed literature survey about the tension leg platform technology and about the tension leg platforms that are already installed or being installed
- To determine the dynamic responses of a typical triangular tension leg platform subjected to different water depths by assuming the platform as a rigid body and by solving the dynamic equations in frequency domain and in time domain

### **1.4 Scope of Study**

- Study on the concepts of a functional TLP. The characteristics, the response of TLP are to be studied.
- Study on the history of TLP installation in the oil and gas production in many places in the world.
- Study on the wave theories, wave parameters and distinguish the suitability of different types of wave theories
- Conduct dynamic analysis of triangular TLP in frequency domain and in time domain
- Determine the effect of varying water depths on the dynamic responses. This is the primary concern of the overall study.

Study is subjected to certain assumptions, as to be mentioned in the following:

- Study will only involve deep water. Intermediate and shallow water are not being considered in the research.
- Dimensional platform (draught, diameter of member, height, etc) and environmental data (wave height, significant height, etc) were assumed to certain values, but based on real dimensional platform and site condition.
- Symmetrical direction of force (horizontal force) is acting on the cylindrical member.
- Vertical forces are zero and assumed to be resisted by the tensile tendons of TLP.
- There are no effects of wind speed in the study.

## CHAPTER 2

### *LITERATURE REVIEW*

Tension-leg platform (TLP) is a floating structure, vertically moored to the seafloor by a system of pre-tensioned tendons held in tension by the buoyancy of the hull. It is a common in the oil and gas production, functions as working stations for oil and gas exploration. Typical picture of a TLP is shown in Figure 2.0. TLP is implemented particularly in deep water production where fixed platforms are less cost-effective. It consists of floating body, pontoons and a top working platform, anchored on the seabed by tendons. Hull provides buoyancy, for support both of weight and to provide tendon tension. Ballast is used to even loading between tendons and to offset unused payload capacity. [2, 6]

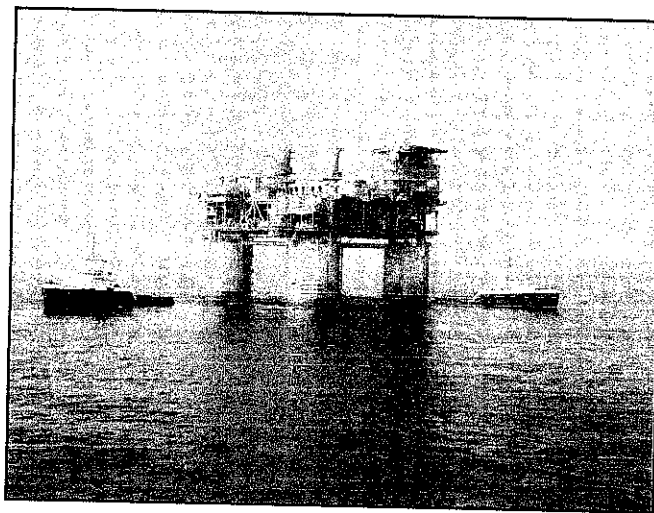


Figure 2.0: Tension Leg Platform [7]

As to date, tension-leg platform has been long recognized as a solution for deepwater production. Size, spacing and submergence of columns and pontoons are major factors in hydrodynamic performance of TLP. Design of the tendon systems is an important part of the overall design of TLP concept. A two dimensional diagram of TLP components is shown below in Figure 2.1 [2]

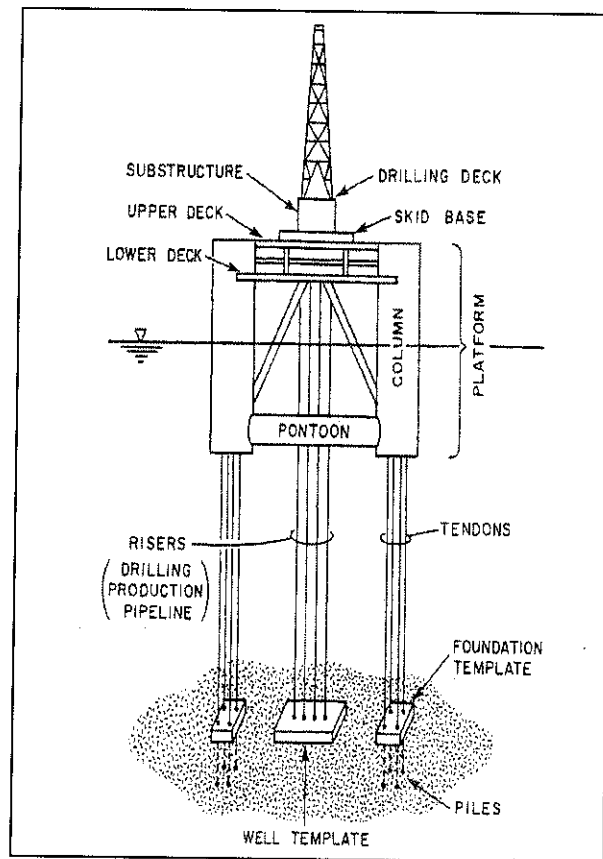


Figure 2.1: Tension leg platform (TLP) components [2]

Today, oil and gas exploration in water depths in excess of 300m (1,000ft) is considered to be deepwater and there are currently 15 rigs in the Gulf of Mexico drilling in over 1,500m (5,000ft) of water. According to the US Department of the Interior Service Deepwater Gulf of Mexico 2007 Report, there are over 4,200 active leases in deepwater with over 650 of these in water depths in excess of 2,200m (7,500ft). [3]

TLPs have been successfully deployed in water depths approaching 1240m (4,000 feet). The first TLP was installed in August 1985 in the Hutton field of the North Sea by Conoco. The TLP consists of a rectangular floating platform connected to the seabed by 16 vertical tendons, four per corner column. Several concepts for TLPs were developed years later to suit the milder environment in Gulf of Mexico. Most of all TLPs in the late 1990s were built using square 4-column units. Three columns have been proposed, but not built. Since the late 1990s, 4 single-column designs (*Sea Star*) and 2 multi-column designs (*Moses*) have been built. [2]

A new development from Atlantia extends the SeaStar TLPs depth capability to 10,000 ft, making it the most economical structure for dry-tree production from ultra-deepwater fields. This new invention introduces water-column oscillators to the hull. These completely passive devices effectively eliminate wave-induced resonant motions and thereby reduce tension and stresses in the tubular tendons. Since tendon walls can now be made thinner, tendon cost is dramatically lowered and is no longer a limiting factor in deeper waters. [2]

The SeaStar monocolumn hull with three radial pontoons is one of the most refined buoyant shapes ever designed. A 3-D drawing of SeaStar TLP is shown in Figure 2.2. The structure is optimized to deliver the maximum payload capacity for a given hull weight. A SeaStar hull supports up to 1.8 times its own weight. By comparison a spar hull supports only about 0.6 times its weight. That means a spar hull contains about three times the steel in a SeaStar hull, which is one of the reasons SeaStar TLPs are more economical than spars. [8]

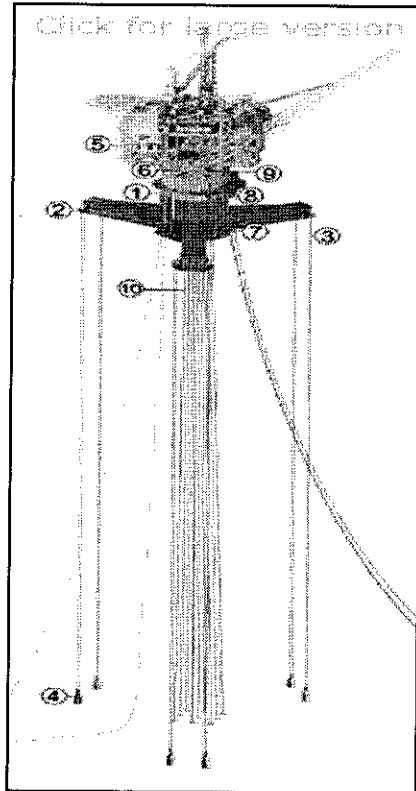


Figure 2.2: SeaStar Tension Leg Platform [8]

Apart from SeaStar, there are many TLPs installed elsewhere in the world. For instance; Brutus TLP. Located in the deep water of Gulf of Mexico, Brutus TLP by Shell was installed in 925m (2985 ft) in 2001. Total project cost was about USD800m, including pipelines. About 70 percent of the costs were associated with fabrication and installation of hull, deck, facilities, drilling rig and pipeline. The rest were related to drilling and completion of the wells. The dimensions of the triangular TLP and the environmental data will be mentioned in the later part of the report. Brutus TLP picture is shown in Figure 2.3. Additional information regarding Brutus TLP is as attached in Appendix D. [9]

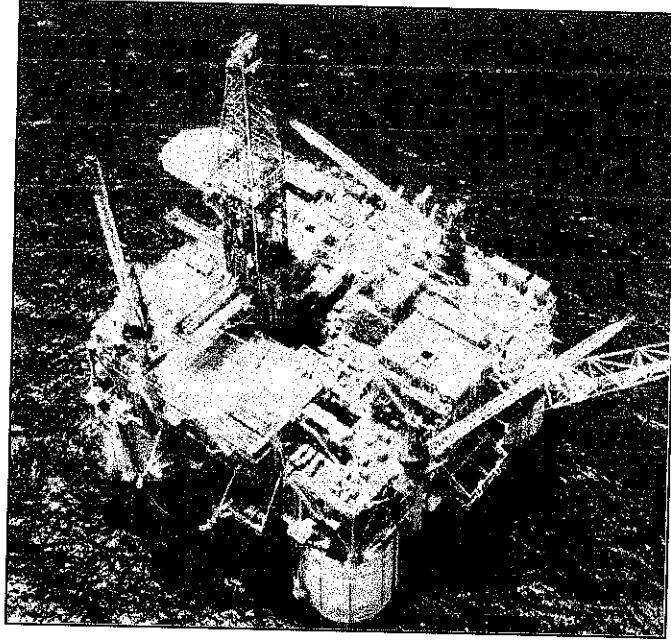


Figure 2.3: Brutus TLP in Gulf of Mexico [9]

In order to study the effect of water depth on the responses of TLP, a series of computation are performed. One of the formulas used is Linear Airy Wave Theory. The following would be the parameters related to Linear Airy Wave Theory:

The horizontal velocity is:

$$u = \frac{\pi H}{T} \frac{\cosh ks}{\sinh kd} \cos \Theta \quad [2]$$

The vertical velocity is:

$$v = \frac{\pi H}{T} \frac{\sinh ks}{\sinh kd} \sin \Theta \quad [2]$$

The horizontal acceleration is:

$$\frac{\partial u}{\partial t} = \frac{2\pi^2 H}{T^2} \frac{\cosh ks}{\sinh kd} \sin \Theta \quad [2]$$

The vertical acceleration is:

$$\frac{\partial v}{\partial t} = -\frac{2\pi^2 H \sinh ks}{T^2 \sinh kd} \cos \Theta \quad [2]$$

Where,

- $\Theta$  = Crest angle, °
- $H$  = Wave height, m
- $T$  = Wave period, s
- $k$  = No. of wave, 1/m
- $s$  = Distance from seabed to analyzed position, m
- $d$  = Water depth, m

For the purpose of wave forces measurement, Morison equation is used. The equation was developed by Morison, O' Brien, Johnson and Shaaf (1950). The Morison equation assumes the force to be composed of inertia and drag forces linearly added together. The components involve an inertia coefficient and a drag coefficient which must be determined experimentally. The Morison equation is applicable when the drag force is significant. This is usually the case when a structure is small compared to the water wave length. [2]

Morison equation is applied by implementing the following formula:

$$dfI = C_M \rho \frac{\pi}{4} D^2 \frac{\partial u}{\partial t} ds \quad [2]$$

$$dfD = 0.5 C_D \rho D |u| u ds$$

Where,

$$\text{Force, } F = \text{Inertia force, } dfI + \text{Drag force, } dfD \quad [2]$$

$C_M$	= Inertia coefficient
$C_D$	= Drag coefficient
$\rho$	= Sea water density, kg/m <sup>3</sup>
$D$	= Diameter of hull, m
$\partial u / \partial t$	= Acceleration of sea water particle, m/s <sup>2</sup>
$u$	= Velocity of sea water particle, m/s
$\partial s$	= Length of segment of structure, m

In 1964, Pierson and Moskowitz proposed a new formula for an energy distribution of a wind generated sea state based on more accurate recorded data. This spectrum which is commonly known as P-M spectrum model had been used extensively all over the world in offshore studies. The P-M spectral model describes developed sea determined by wind speed. The spectrum based on assumptions that wind has to blow over a large area at a closely constant speed for many hours to time when wave record is obtained without significant change of wind direction. [2]

The equation for P-M spectrum is:

$$S(f) = \alpha g^2 / (2\pi)^4 f^5 \exp[-1.25(f/f_0)^{-4}] \quad [2]$$

Where,

$$\alpha = 0.0081$$

$$g = 9.81 \text{ m/s}^2$$

$$\pi = 3.142$$

$f$  = frequency of waves, Hz

$f_0$  = peak frequency of waves, Hz

The height of a wave is required at a particular frequency from the energy density spectrum. It is to be applied to compute the forces acting upon TLP and the responses of the structure. The wave height,  $H$  is obtained using the following formula:

$$H(f) = 2\sqrt{2S(f)\Delta f} \quad [2]$$

Where,

$S(f)$  = Wave spectrum,  $m^2s$

$f$  = Wave frequency, Hz

Wave profile can be computed from the formula:

$$\eta(x,t) = \sum (H(n)/2) \cos[k(n)x - 2\pi f(n)t + \varepsilon(n)] \quad [2]$$

Where,

$k$  = No. of wave,  $1/m$

$x$  = horizontal coordinate, m

$t$  = time, s

$f$  = Wave frequency, Hz

$\varepsilon(n) = 2\pi R_N$  ( $R_N$  is random number, ranged from 0 to 1)

Numerous works had been carried out to study the parameters of deep water, to compute the amount of forces acting upon an offshore structure, and to calculate the energy of random waves at sea. Surge, heave and pitch analysis were carried out to analyze the responses of the TLP upon varying water depth.

## **CHAPTER 3**

### ***METHODOLOGY***

The project initiates with intense researches of many TLPs installation through out the world, and studies of a functional TLP. Next, once the basic foundation of a TLP is known, wave theory is implemented to study several parameters (displacements, velocities, accelerations, etc) related to water depth. For this purpose, Linear Airy Wave Theory is applicable, with the assumption that the wave height is small compared to the wave height or water depth.

The other approach is to study waves is by using the wave spectrum. Random waves are correlated to ocean waves. Study applies the Pierson-Moskowitz (P-M) Spectrum because this model gives a rather more accurate recorded data. By using P-M spectrum model, the total energy of a random wave at sea can be computed and analyzed. Morison equation assumes the force to be composed of inertia and drag forces. The equation is used when drag force is significant.

Application of Morison equation together with Response Motion Spectrum is used to study motion responses acting on a TLP which are the surge, heave and pitch.

### **3.1 Research**

Numerous researches were carried out in the study in order to gain as much information as possible to begin with. The scopes of researches are concerning about the history of TLPs installation of the world and dimensional platforms and environmental data.

The required data are shown as follow:

- a) Dimensional Platform
  - i) Plan Dimension
  - ii) Height
  - iii) Draught
  - iv) Centre of Gravity position
  - v) Radii of Gyration
  - vi) Tethers
  - vii) Mass / Weights
  
- b) Environmental Data
  - i) Water Depth
  - ii) Wave Height
  - iii) Wave Length
  - iv) Significant Height

### **3.2 Conduct Analysis**

The displacement of the hull and the axial stiffness of the vertical tendons are chosen such that the vertical natural periods are short and the horizontal natural periods are long. Minimum vertical motion reduces the complexity of well system consequently. Several water wave theories have been developed and are applicable to different environments, depending on the three main parameters; water depth, wave height and wave period. As for the study, Linear Airy Wave Theory is to be used, considering the three main parameters and assuming that the wave height is small compared to the wave length or water depth. This wave theory which is also known as sinusoidal wave theory is based on the assumption that the wave height is small compared to wave length or water depth.

From the data gained, several analyses will be conducted. The dynamic equations in frequency domain and in time domain will also be studied. For that purpose, P-M Spectral Model was used to study the wave energy density spectrum of random waves. Dynamic responses of the typical triangular TLP subjected to random wave loads will be analyzed by assuming the platform as a rigid body. Surge analysis had been conducted in the Final Year Project 1. Heave and pitch analysis had been analyzed during Final Year Project 2, including the study of varying water depth on TLP responses. Project methodology diagram will be shown in Figure 3.0.

### **3.3 Software required**

The softwares required in the project are:

- a) Microsoft Excel
- b) MatLab (Optional)
- c) SACS (Optional)

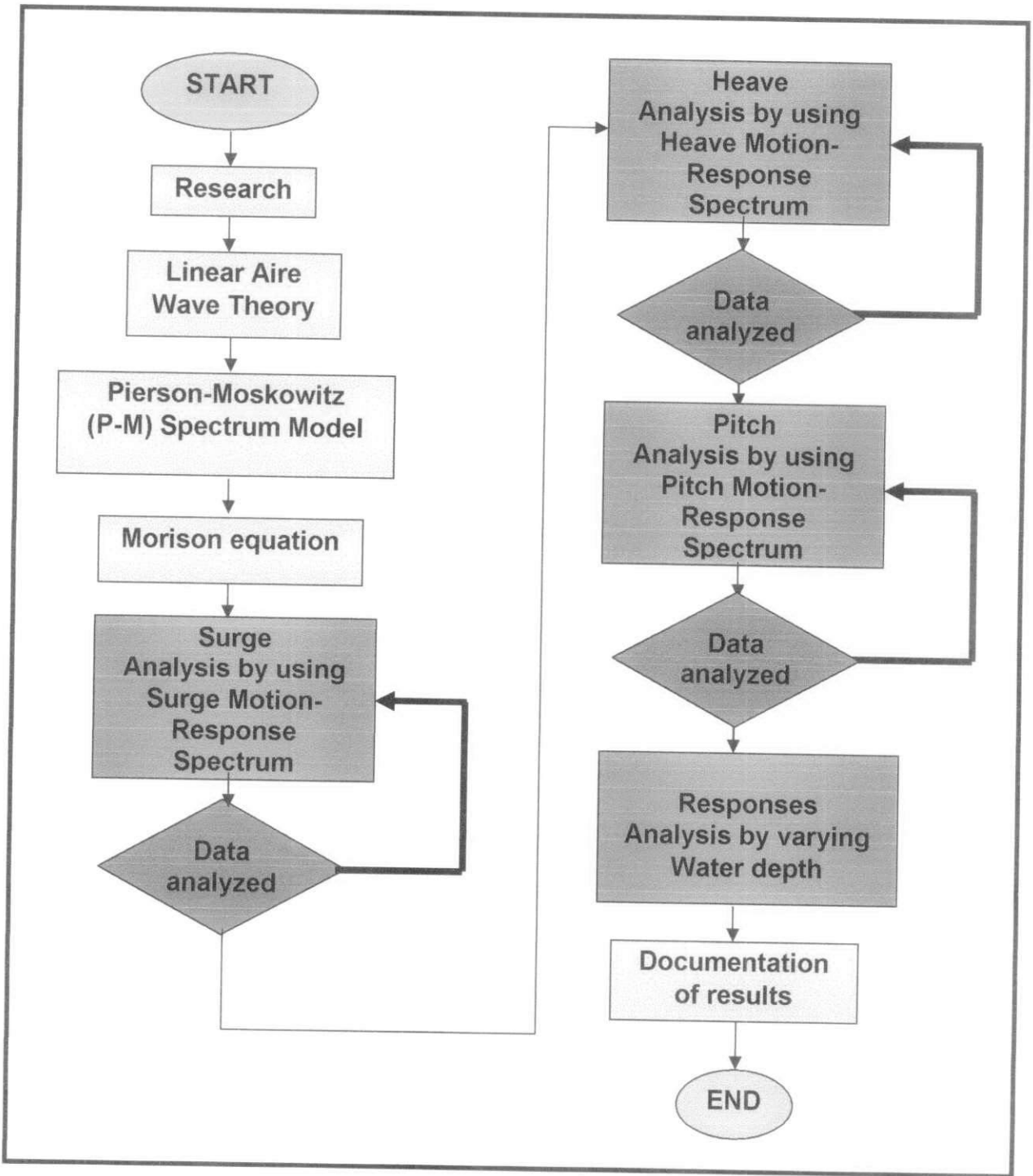


Figure 3.0: Project methodology diagram

### **3.4 Health, Safety & Environment (HSE) Analysis**

The offshore lab of UTP had been visited on several occasions on this semester. There were some Health, Safety, & Environment (HSE) aspects during the lab session. The HSE aspects are important, to ensure safeness and to avoid any casualties. The HSE aspects are as follows:

1. Wear lab coat during the lab session.
2. Avoid walking nearby the pond when stepping on the stairs.
3. Avoid littering into the pond and flume.
4. Avoid smoking in the lab.
5. Listen to any instruction given by the laboratory assistant or the lecturer.

## CHAPTER 4

### RESULTS AND DISCUSSIONS

#### 4.1 Dimensional, Structural and Environmental Data

The dimensional, structural and environmental data of the TLP are given as in Figure 4.0:

<b>TLP Dimensional data</b>			
Section	Diameter (m)	Length (m)	Amount
Column	20	40	3
Pontoon	15	50	3
Tendons	0.8	880	12 (4 at each column)

<b>Structural data</b>	
Total mass (tonnes)	42440
Total weight (kN)	416336
Tethers stiffness (kN/m)	102000
Draught (m)	30
Centre of gravity (m)	6.1 (below draught)

<b>Environmental data</b>	
Significant wave height, $H_s$	7.5
Peak frequency, $f$ , (Hz)	0.0730
Drag coefficient, $C_D$	0.65
Mass coefficient, $C_M$	1.6

Figure 4.0: Dimensional and Environmental Data of Case Study TLP [9, 10]

## 4.2 Coordinate system of triangular TLP

Coordinate system for triangular TLP is drawn as in Figure 4.1:

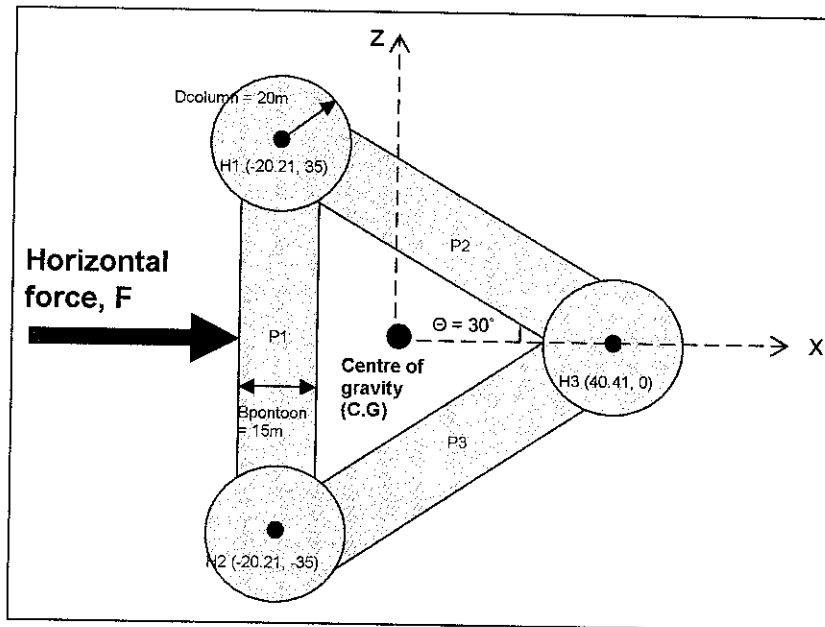


Figure 4.1: Coordinate system for a particular triangular TLP from plan view

Coordinate system as shown in Figure 4.1 represents the position of the TLP. It is assumed that the horizontal force will act perpendicularly upon the pontoon P1.

## 4.3 Analysis on Wave Spectrum

Wave spectrum is used to describe the energy content of an ocean wave and its distribution over a frequency range of the random wave. In order to get the wave spectrum, several mathematical spectrum models are available, such as Scott, ISSC, ITTC, JONSWAP, etc. The most common spectrum, Pierson-Moskowitz (P-M) model is used for the study. P-M spectrum gives more accurate data, applicable in the design of offshore structures, and moreover it is based on single-parameter which is significant wave height,  $H_s$ .

## Pierson Moskowitz Spectrum (P-M)

The following would be the formulations adopted in P-M spectrum:

$$\omega_p^2 = \frac{0.161g}{H_s} \quad [2]$$

$$S(f) = \frac{\alpha g^2}{2\pi^4} f^{-5} \exp[-1.25(f / f_p)^{-4}] \quad (1.0) \quad [2]$$

By inserting value of gravity acceleration,  $g$  and significant wave height,  $H_s$ , the peak frequency,  $f_p$  can be obtained:

$$\omega_p^2 = \frac{0.161(9.81)}{7.5}$$

$$\omega_p = 0.459 \text{ rad / s}$$

Peak angular frequency,  $\omega_p = 2\pi f_p$

Peak frequency,  $f_p = 0.073 \text{ Hz}$

By putting in the values into Equation (1.0), wave spectral density  $S(f)$  value can be obtained by means of varying frequency,  $f$  ranging from 0.035 Hz to 0.275 Hz with an interval of 0.01. A graph of  $S(f)$  versus frequency,  $f$  is plotted as in Figure 4.2:

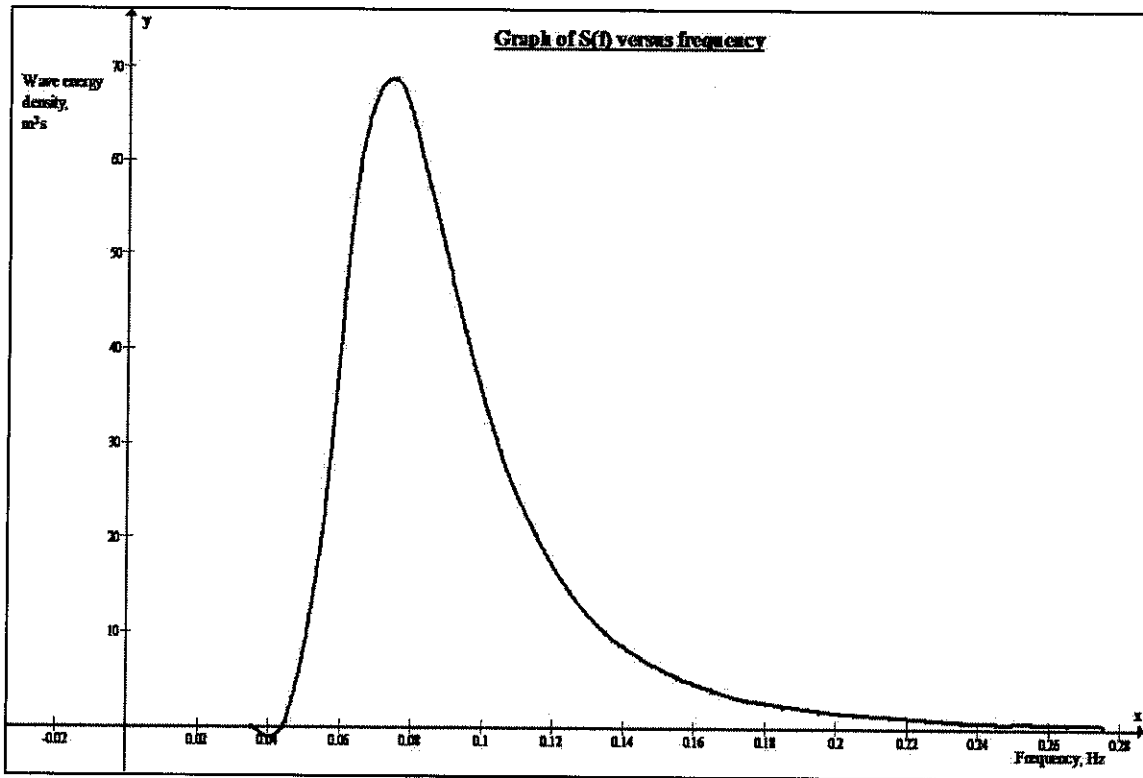


Figure 4.2: Graph of Wave Energy Density Spectrum

Based on Figure 4.2, it can be observed that the maximum value of wave energy density is located at peak frequency,  $f_p = 0.073\text{Hz}$ . It is also noticed that the spectrum generally rises sharply at the low frequency end to a maximum value and decreases gradually with increasing frequency. The area under the curve gives the total energy of the wave system,  $m_s$ , at value of estimation about  $3.5\text{m}^2$ . By applying the formula  $4\sqrt{m_s}$ , the significant height,  $H_s$  of the waves can be computed.

#### 4.4 Analysis of Wave Time Series

From the wave spectrum energy graph, the surface water elevation (also known as wave profile) can be computed. The range of frequency is taken from  $0.35\text{Hz}$  to  $0.275\text{Hz}$ .  $n$  values were taken from random numbers,  $R_N$  which range randomly from 0 to 1. Peak frequency,  $f_p$  is calculated to be  $0.073\text{ Hz}$ , by applying an assumption that the significant wave height is  $7.5\text{m}$ .

Water surface elevation,  $\zeta$  is computed by the following formula:

$$\eta(x,t) = \sum H(n)/2 \cos [k(n)x - 2\pi f(n)t + \varepsilon(n)] \quad (1.1)$$

where  $H(n)$  = wave height

$$k(n) = 2\pi/L(n)$$

$x$  = varying  $x$  coordinate (depending on the location of hull)

Values of the term with  $(n)$  indicate that the values are varying, and depending on range of frequency from 0.35Hz to 0.275Hz.

Phases,  $\varepsilon$  are calculated by using the formula  $\varepsilon(n) = 2\pi RN$ .

After all the values of surface water elevation of Hull 1, Hull 2 and Hull 3 were obtained, they were plotted in graphs as shown in Figure 4.3 and Figure 4.4. Range of time applied for the analysis were taken from  $t=0s$  to  $t=100s$ .

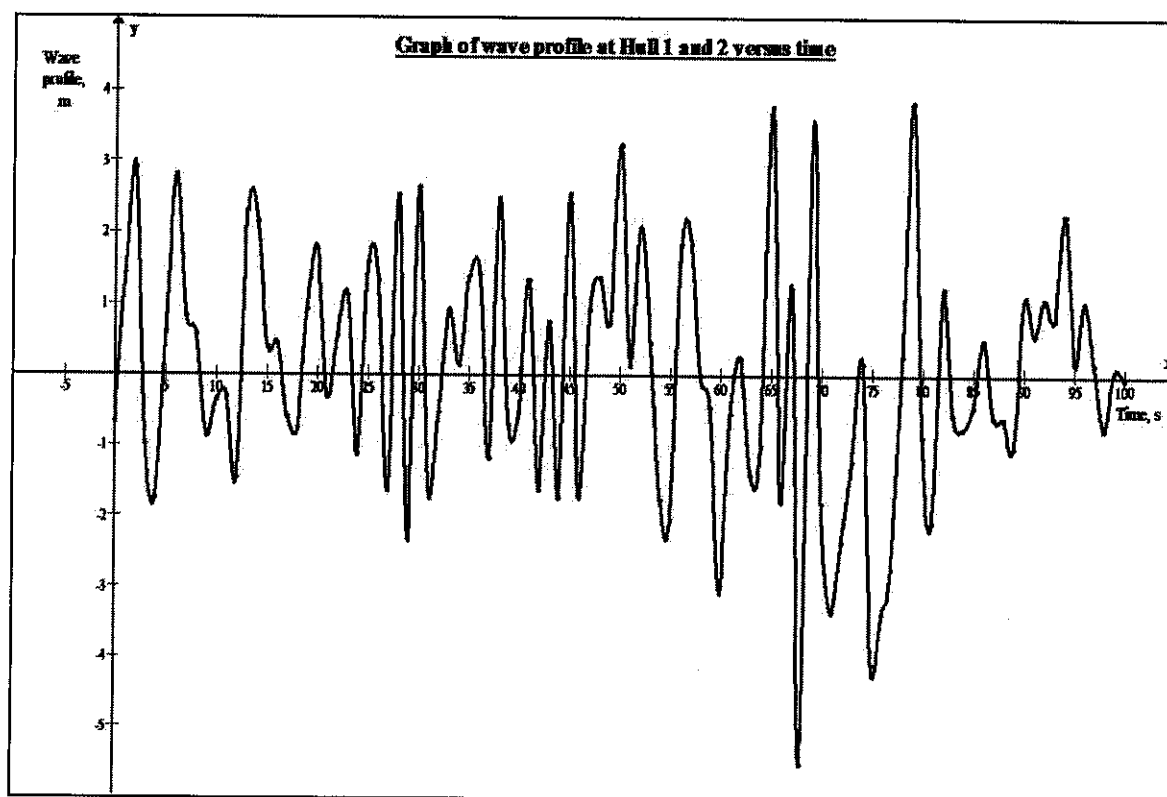


Figure 4.3: Graph of wave profile at Hull 1 and Hull 2

Figure 4.3 presents the wave profile at Hull 2 and Hull 3. It can be observed that the values of elevations were randomly phased from  $t=0s$  to  $t=100s$  and produced wavy shape. The highest elevation is 3.8m at  $t=79s$  while the lowest elevation is 5.5m at  $t=68s$ .

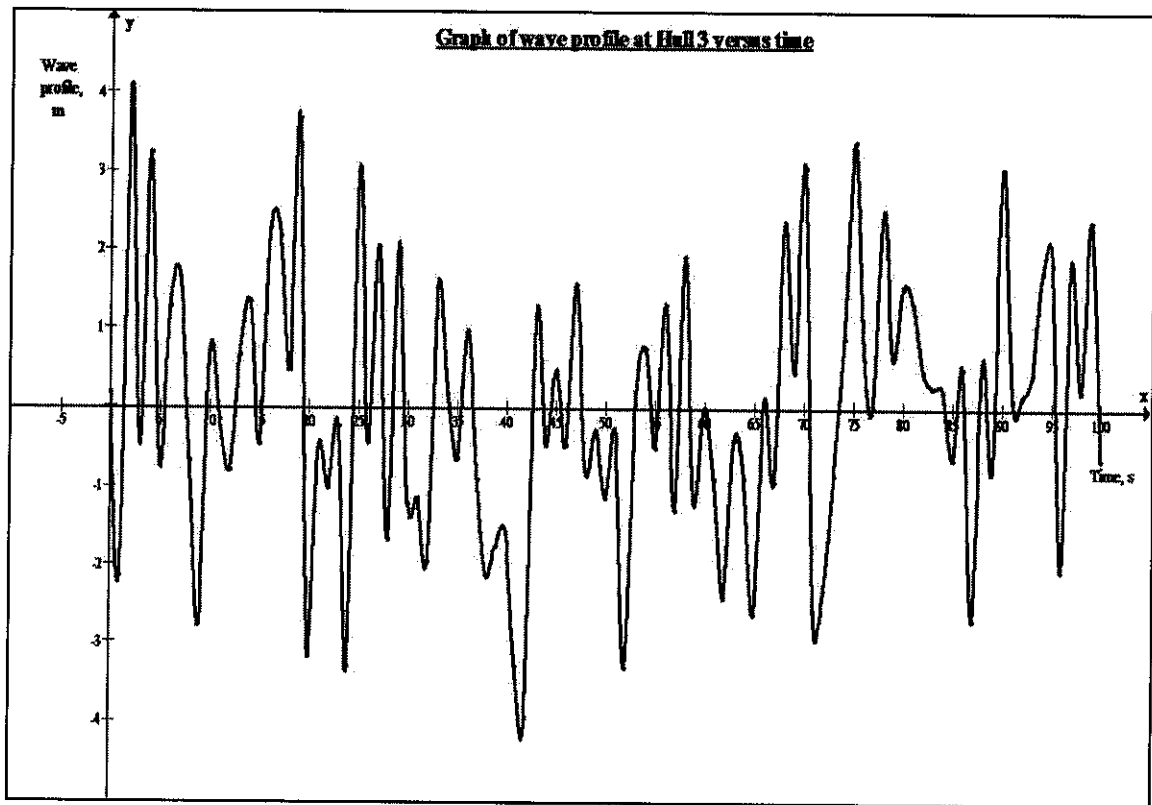


Figure 4.4: Graph of wave profile at Hull 3

Meanwhile, Figure 4.4 above shows the wave profile at Hull 3. It is noted that the highest elevation is 4.09m at  $t=2s$  and the lowest is 3.3m at  $t=41s$ . The result obtained for Hull 1 and Hull 2, compared to Hull 3 is not the same. It is due to the different value of  $x$  in the coordinate system.

Based on Equation (1.1) to calculate surface wave elevation:

$$\zeta(x,t) = \sum H(n)/2 \cos [k(n)x - 2\pi f(n)t + \epsilon(n)]$$

For Hull 1 and Hull 2, the value of  $x$  is -20.21 while for Hull 3,  $x$  is taken as 40.41.

## 4.5 Analysis on surge response

Surge is the movement of TLP along the x axis. The movement is horizontal and it is due to the motion of the ocean waves. Analysis on the surge response of triangular TLP was carried out, considering many parameters such as tendon stiffness, mass of surge, buoyant force, etc.

### 4.5.1 Parameters in surge analysis

#### Mass of Surge

$$\text{Mass of Surge, } M_{\text{SURGE}} = \text{Mass, } M + \text{Added Mass, } M_{\text{ADD}}$$

$$\text{Mass of Structure, } M = 42440000\text{kg}$$

$$\text{Added Mass, } M_{\text{ADD}} = [V_{\text{HULLS}} + V_{P1} + 2(V_{P2,P3} \cos 60^\circ + \frac{\pi D_P^3}{12 \cos 30^\circ})] \times 1030\text{kg} / \text{m}^3$$

=

$$[3 \times \frac{\pi}{4} (20^2)(30) + (15)(50) + 2((15)(50) \cos 60^\circ + \frac{\pi 20^3}{12 \cos 30^\circ})] \times 1030\text{kg} / \text{m}^3$$

$$= 35011\text{m}^3 \times 1030\text{kg} / \text{m}^3$$

$$= 36061330\text{kg}$$

$$M_{\text{SURGE}} = 42440000\text{kg} + 36061330\text{kg}$$

$$= \mathbf{78501330 \text{ kg}}$$

#### Buoyant Force

$$F_{\text{BUOYANCY}} = (V_{\text{HULLS}} + V_{\text{PONTOONS}}) \times 1030\text{kg} / \text{m}^3 \times 9.806\text{m} / \text{s}^2 / 1000$$

$$= (28274.33 + 26507.19) \text{m}^3 \times 10.10018\text{kg} / \text{m}^2\text{s}^2$$

$$= \mathbf{553303.2\text{kN}}$$

#### Surge Stiffness (for 900m water depth calculation only)

$$\text{Buoyancy, } B = \text{Structure weight in air, } W + \text{Tethers tension, } T$$

$$B = 553303.2 \text{ kN}$$

$$W = 416336.4 \text{ kN}$$

$$T = B - W$$

$$= 136966.8 \text{ kN}$$

$$\text{Tether length, } L = 880\text{m}$$

$$\begin{aligned} K_{\text{SURGE}} &= T/L \\ &= 136966.8 \text{ kN}/880\text{m} \\ &= \mathbf{155.644\text{kN/m}} \end{aligned}$$

The results of calculation of surge parameters for all the water depths will be as attached in Appendix A.

#### 4.5.2 Calculation of surge response

TLP will produce responses when subjected to a random wave of given frequency. The amplitude of the response is basically has correlation with the amplitude of the wave. If a response function is built for a range of wave frequencies for TLP, this function is named the Response-Amplitude Operator (RAO). RAO allows the transformation of waves into the responses of the structure.

$$\text{Surge response (t)} = RAO_{\text{SURGE}} \times \eta(t) \quad (1.2)$$

where  $\eta(t)$  is the wave profile as mentioned earlier in section 4.4.

$$RAO_{\text{SURGE}} = \left[ \frac{F / \left( \frac{H}{2} \right)}{(K - m\omega^2)^2 + (C\omega^2)^2} \right]^{\frac{1}{2}} \quad (1.3)$$

Where,	F	=	Total horizontal force, kN
	H	=	Wave height, m
	K	=	Surge stiffness, kN/m
	C	=	Damping, $2\zeta m \omega_n$ where $\zeta=0.01$
	m	=	Mass plus added mass, kg

Furthermore,  $RAO_{SURGE}$  relates surge motion of TLP to the wave-forcing function on the structure. Surge-response spectrum  $S(f)_{SURGE}$  is obtained from the wave spectrum,  $S(f)$ .

The equation is as the following:

$$S(f)_{SURGE} = [RAO_{SURGE}]^2 \times S(f) \quad (1.4)$$

Graphs of  $RAO_{SURGE}$  and  $S(f)_{SURGE}$  versus frequency are shown in Figure 4.5 and Figure 4.6.

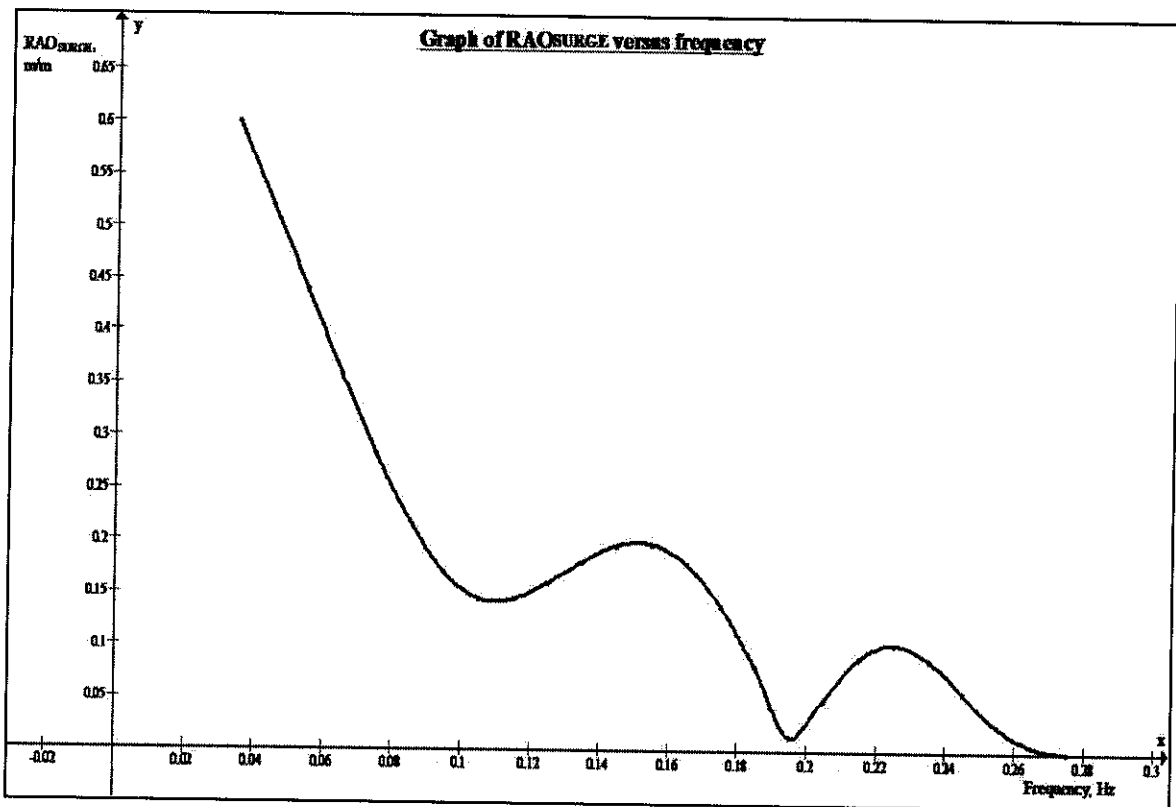


Figure 4.5: Graph of  $RAO_{SURGE}$

Figure 4.5 shows the  $RAO_{SURGE}$  versus frequency. From the graph plotted, it is observed that  $RAO_{SURGE}$  is highest at lowest frequency,  $f$  which is at 0.035Hz. Based on Equation

(1.3), when the values of wave height,  $H$  and angular frequency,  $\omega$  become smaller, the  $RAO_{SURGE}$  value will increase significantly.

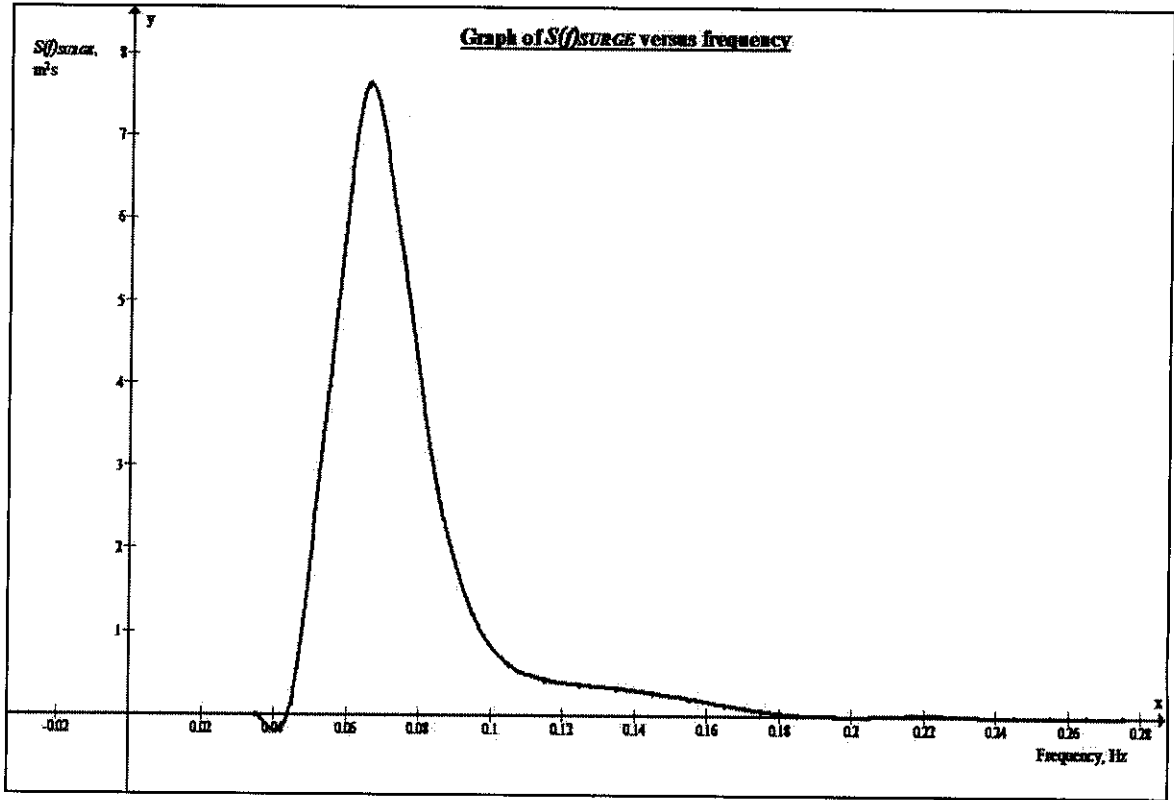


Figure 4.6: Graph of surge spectrum,  $S(f)_{SURGE}$  versus frequency

$S(f)_{SURGE}$  as plotted in Figure 4.6 has a maximum peak value corresponding to the wave-spectral peaks, but also has additional peaks. Area under the curve was calculated, giving a value of  $0.24\text{m}^2$ . The peaks are subjected to the power of two of  $RAO_{SURGE}$  multiplied by  $S(f)$  in Equation (1.4). The surge responses at Hull 1, Hull 2 and Hull 3 versus series of time of 100s are plotted in the Figure 4.7 and Figure 4.8.

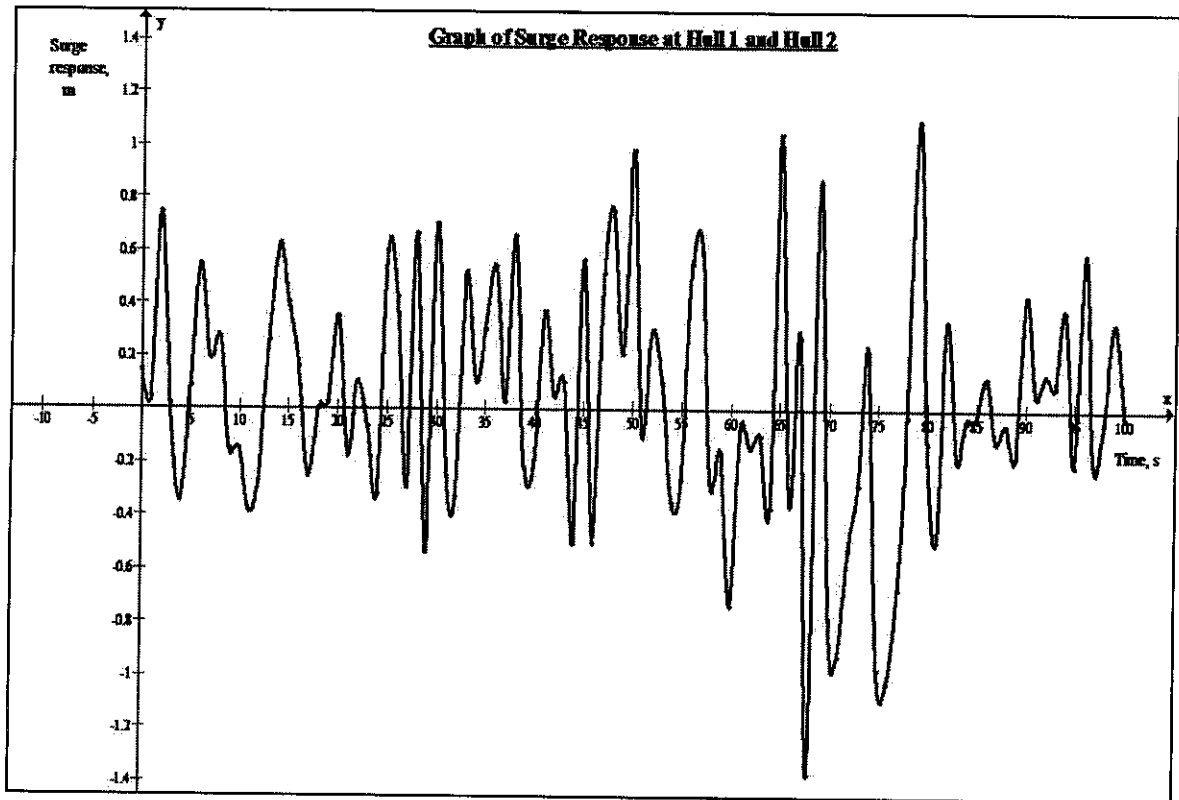


Figure 4.7: Graph of surge response at Hull 1 and Hull 2

Figure 4.7 shows that the surge response at Hull 1 and Hull 2. Positive surge response indicates that the surge is moving on x axis to the right, induced by horizontal force. Negative surge response on the other hand indicates that the surge is moving backwards. Positive movement of the surge is slightly less significant than the negative surge response. Maximum value of positive surge response is 1.16m at  $t=78s$  while the maximum for negative surge response is 1.4m at  $t=67s$ .

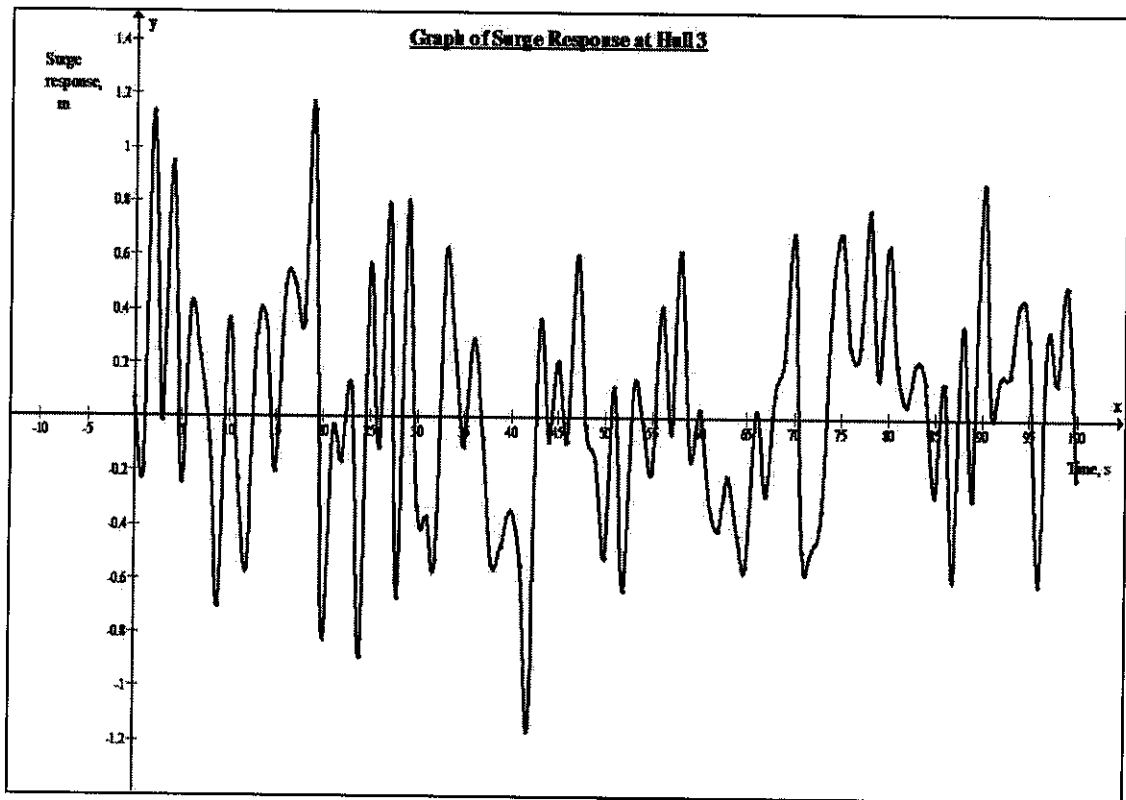


Figure 4.8: Graph of surge response at Hull 3

Meanwhile, Figure 4.8 shows the surge response at Hull 3. From the graph, positive movement of the surge is having larger response than the negative surge. Maximum value of positive surge response is 1.1m at  $t=19s$  while the maximum for negative surge response is 1.1m at  $t=42s$ .

## 4.6 Analysis on heave response

Heave is the movement of TLP along the y axis. The movement is vertical and it is due to the vertical forces and dynamic bottom pressure acting upon the hulls. Analysis on the heave response of triangular TLP was carried out, considering many parameters such as heave stiffness, mass of heave, upward pressure, etc.

### 4.6.1 Parameters in heave analysis

#### Mass of Heave

$$\text{Mass of Heave, } M_{\text{HEAVE}} = \text{Mass, } M + \text{Added Mass, } M_{\text{ADD}}$$

$$\text{Mass of Structure, } M = 42440000 \text{ kg}$$

$$\begin{aligned} \text{Added Mass, } M_{\text{ADD}} &= 3\rho \left[ \frac{\pi D_c^3}{12} + \frac{\pi D_p^2}{4} \right] \\ &= 3 \times 1030 \text{ kg/m}^3 \times \left[ \frac{\pi 20^3}{12} + \frac{\pi 15^2}{4} \right] \end{aligned}$$

$$= 33774085 \text{ kg}$$

$$M_{\text{HEAVE}} = M + M_{\text{ADD}}$$

$$= 42440000 \text{ kg} + 33774085 \text{ kg}$$

$$= \mathbf{76214085 \text{ kg}}$$

#### Bottom Dynamic Pressure

The bottom dynamic pressure is obtained by using the following formula:

$$p = \rho g \frac{H \cosh ks}{2 \cosh kd} \cos \Theta \quad [2]$$

### Stiffness in Heave

$K_{HEAVE}$  is computed using the following formula:

$$= 3\left[\left(\frac{\pi}{4} D^2 \rho_w g\right) + \frac{AE}{L}\right]$$

Where  $\frac{AE}{L} = K_{TETHER} = 102000 \text{ kN/m}$

$$= 3\left[\left(\frac{\pi}{4} \times 20^2 \times 1030 \times 9.81\right) + 102000\right]$$

$$= 315523 \text{ kN/m}$$

The results of calculation of heave parameters for 900m water depth will be as attached in Appendix B. Only 900m heave parameters is attached since heave parameters do not change with changing water depth.

#### **4.6.2 Calculation of heave response**

TLP will produce responses when subjected to a random wave of given frequency. The amplitude of the response is basically has correlation with the amplitude of the wave. If a response function is built for a range of wave frequencies for TLP, this function is named the Response-Amplitude Operator (RAO). RAO allows the transformation of waves into the responses of the structure.

$$\text{Heave response (t)} = RAO_{HEAVE} \times \eta(t) \quad (1.5)$$

Where  $\eta(t)$  is the wave profile as analyzed in previous section in 4.4

$$RAO_{HEAVE} = \left[ \frac{F \left( \frac{H}{2} \right)}{(K - m\omega^2)^2 + (C\omega^2)^2} \right] \quad (1.6)$$

Where, F = Total vertical force, kN  
H = Wave height, m

- K = Heave stiffness, kN/m
- C = Damping,  $2\zeta m \omega_n$ , where  $\zeta=0.01$
- m = Mass plus added mass, kg

Furthermore,  $RAO_{HEAVE}$  relates surge motion of TLP to the wave-forcing function on the structure. Heave-response spectrum,  $S(f)_{HEAVE}$  is obtained from the wave spectrum,  $S(f)$ .

The equation is as the following:

$$S(f)_{HEAVE} = [RAO_{HEAVE}]^2 \times S(f) \quad (1.7)$$

Graphs of  $RAO_{HEAVE}$ , and  $S(f)_{HEAVE}$  versus frequency are as shown in Figure 4.9 and Figure 4.10.

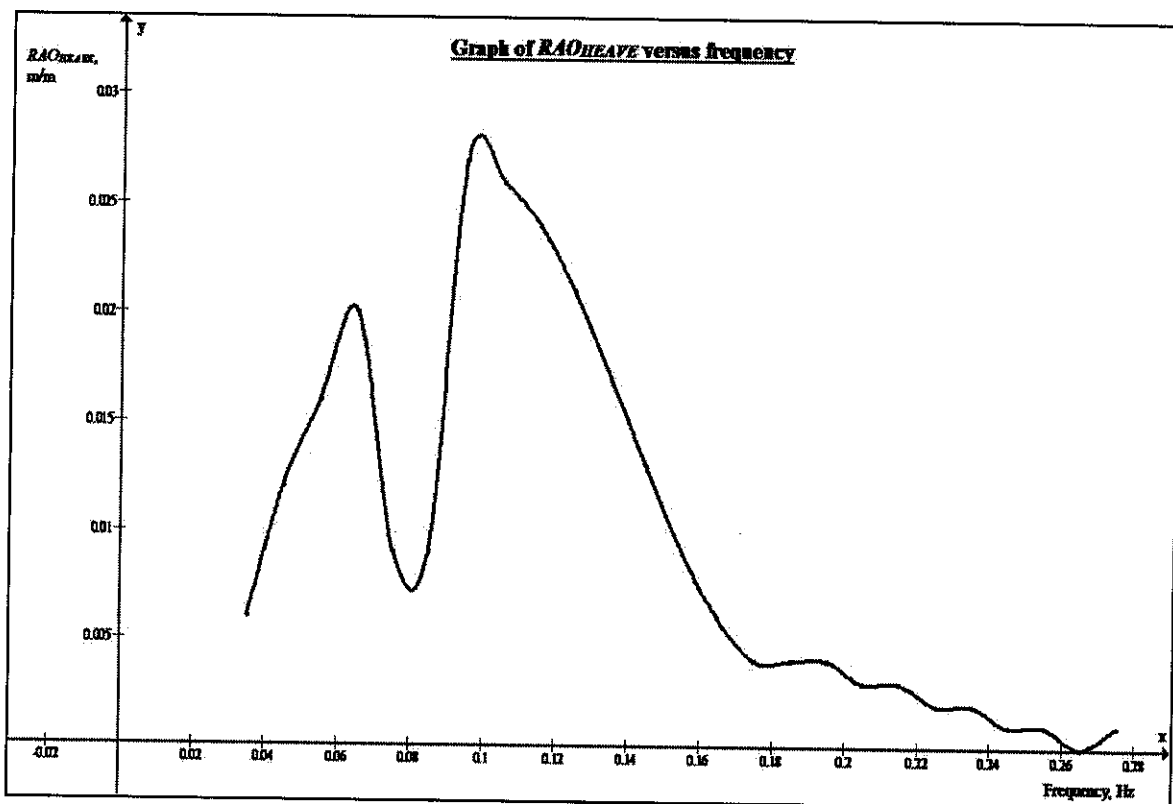


Figure 4.9: Graph of  $RAO_{HEAVE}$  versus frequency

Figure 4.9 shows that the  $RAO_{HEAVE}$  value is highest when the frequency,  $f$  is at 0.1Hz. This is because the wave height,  $H$  at frequency 0.1Hz is small. Based on Equation (1.6), when the value of wave height,  $H$  or angular frequency,  $\omega$  becomes smaller, the  $RAO_{HEAVE}$  value will increase significantly.

There are few peaks in the  $RAO_{HEAVE}$ ; at  $f=0.06\text{Hz}$ ,  $f=0.1\text{Hz}$ . These peaks are caused by the wave lengths which correspond to the frequencies.

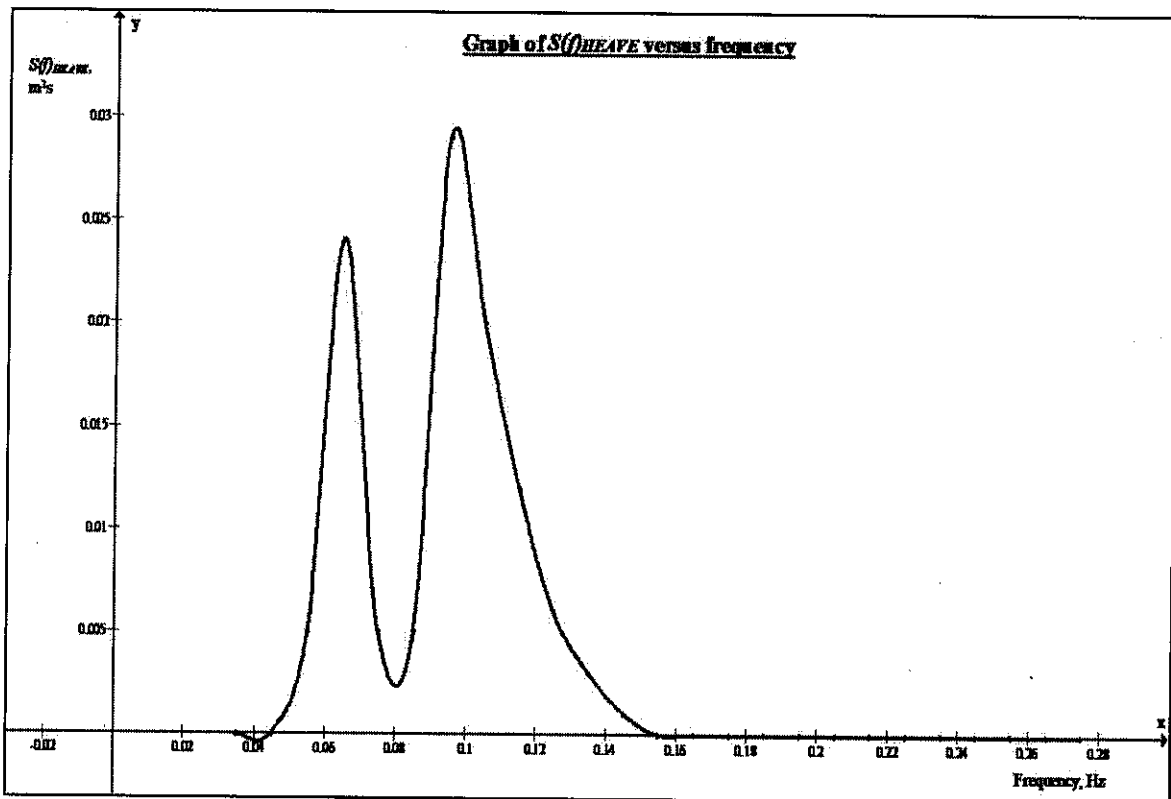


Figure 4.10: Graph of heave spectrum,  $S(f)_{HEAVE}$  versus frequency

Heave spectrum as plotted in Figure 4.10 has a maximum peak of  $0.029\text{m}^2\text{s}$  and additional peak of  $0.024\text{m}^2\text{s}$ . The peaks are subjected to the power of two of  $RAO_{HEAVE}$  multiplied by  $S(f)$  in Equation (1.7). Area under the  $S(f)_{HEAVE}$  was computed, giving a value of  $0.001\text{m}^2$ .

The heave responses at versus series of time of 100s are as shown in Figure 4.11.

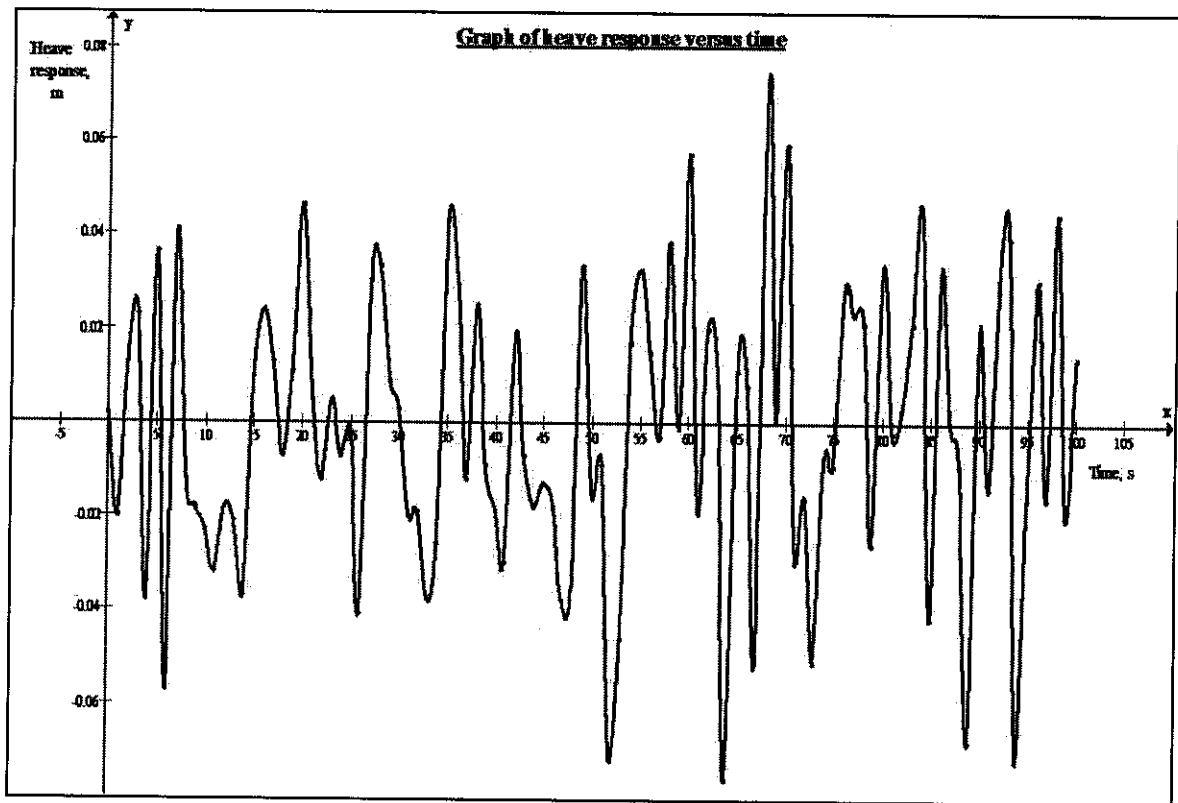


Figure 4.11: Graph of heave response versus time

Positive heave response indicates that the heave is moving on y axis vertically, induced by vertical force. Negative heave response on the other hand indicates that the heave is moving downwards. Figure 4.11 points out that positive heave response gives values generally around 0.02-0.04m while negative heave response produces values around 0.04m. Maximum value of positive heave response is 0.08m at  $t=63s$  while the maximum for negative heave response is 0.076m at  $t=64s$ .

## 4.7 Analysis on pitch response

Pitch is the movement of rotation of TLP along the z axis. The movement is rotating and it is due to the horizontal forces acting upon TLP. Analysis on the pitch response of triangular TLP was carried out, considering many parameters such as surge mass, centre of gravity, etc.

### 4.7.1 Parameters in pitch analysis

#### Mass of Pitch

Mass of Pitch,  $M_{PITCH}$  = Mass of Surge,  $M_{SURGE}$  x Radius of gyration  
(x axis)

$$\begin{aligned} M_{PITCH} &= (M_{SURGE})r_{xx}^2 \\ &= 78501330 \text{ kg} \times 40.41\text{m}^2 \\ &= 128190167698 \text{ kgm}^2 \end{aligned}$$

#### Stiffness in Pitch

$T_n$  for pitch is selected as 2s.

$K_{PITCH}$  is computed using the following formula:

$$\omega_n = \sqrt{\frac{K_{pitch}}{M_{pitch}}} \quad [2]$$

$$\begin{aligned} K_{PITCH} &= \omega_n^2 M_{PITCH} \\ &= 1265186243\text{kNm/rad} \end{aligned}$$

The results of calculation of pitch parameters for 900m water depth will be as attached in Appendix C. Only 900m pitch parameters is attached since pitch parameters do not change with changing water depth.

#### 4.7.2 Calculation of pitch response

TLP will produce responses when subjected to a random wave of given frequency. The amplitude of the response is basically has correlation with the amplitude of the wave. If a response function is built for a range of wave frequencies for TLP, this function is named the Response-Amplitude Operator (RAO). RAO allows the transformation of waves into the responses of the structure.

$$\text{Pitch response (t)} = RAO_{PITCH} \times \eta(t) \quad (1.8)$$

where  $\eta(t)$  is the wave profile as analyzed in previous section in 4.4

$$RAO_{PITCH} = \left[ \frac{F / \left( \frac{H}{2} \right)}{(K - m\omega^2)^2 + (C\omega^2)^2} \right]^{\frac{1}{2}} \quad (1.9)$$

Where ,	F	=	Total moment, Nm
	H	=	Wave height, m
	K	=	Pitch stiffness, Nm/rad
	C	=	Damping, $2\zeta m \omega n$ , where $\zeta=0.01$
	m	=	Mass of pitch, $\text{kgm}^2$

Furthermore,  $RAO_{PITCH}$  relates pitch motion of TLP to the wave-forcing function on the structure. Pitch-response spectrum,  $S(f)_{PITCH}$  is obtained from the wave spectrum,  $S(f)$ .

The equation is as the following:

$$S(f)_{PITCH} = [RAO_{PITCH}]^2 \times S(f) \quad (2.0)$$

Graphs of  $RAO_{PITCH}$ , and  $S(f)_{PITCH}$  versus frequency are shown in Figure 4.12 and Figure 4.13.

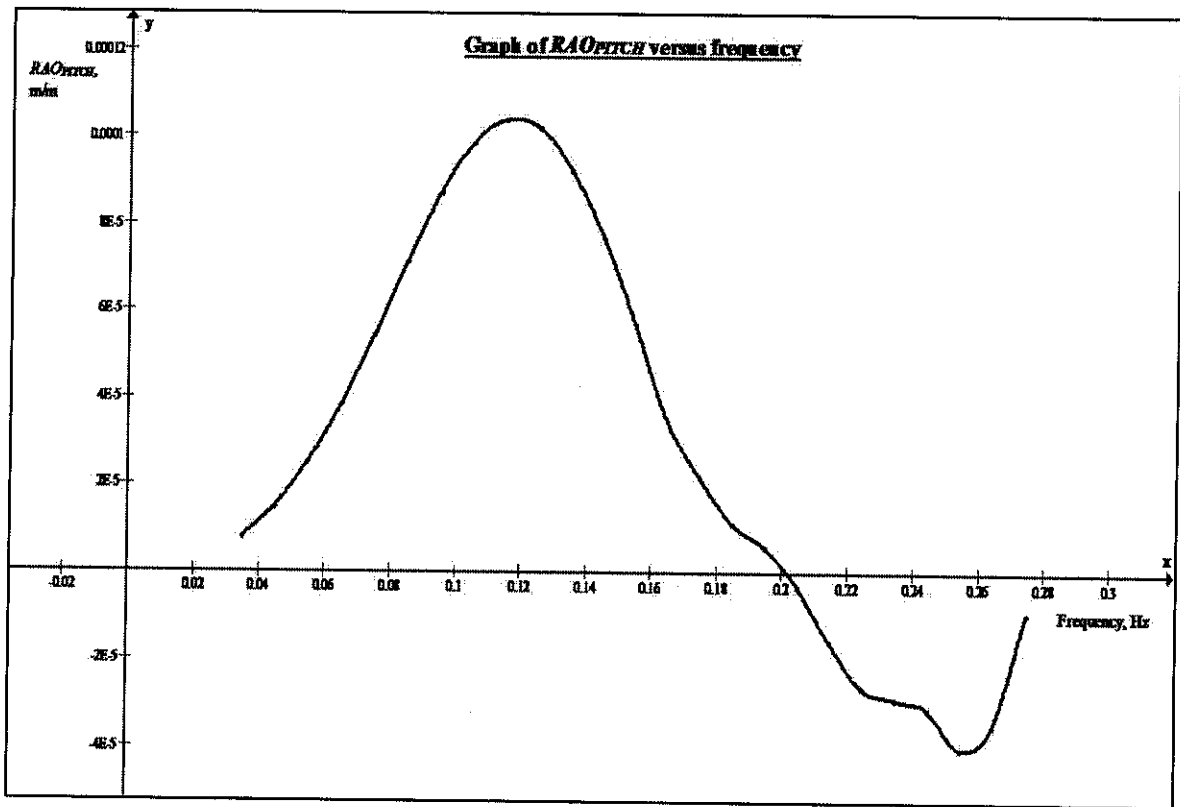


Figure 4.12: Graph of  $RAO_{PITCH}$  versus frequency

Figure 4.12 shows that the  $RAO_{PITCH}$  value is at the highest 0.000104 when at frequency 0.115Hz. The lowest  $RAO_{PITCH}$  is 0.00004 at frequency 0.255Hz.

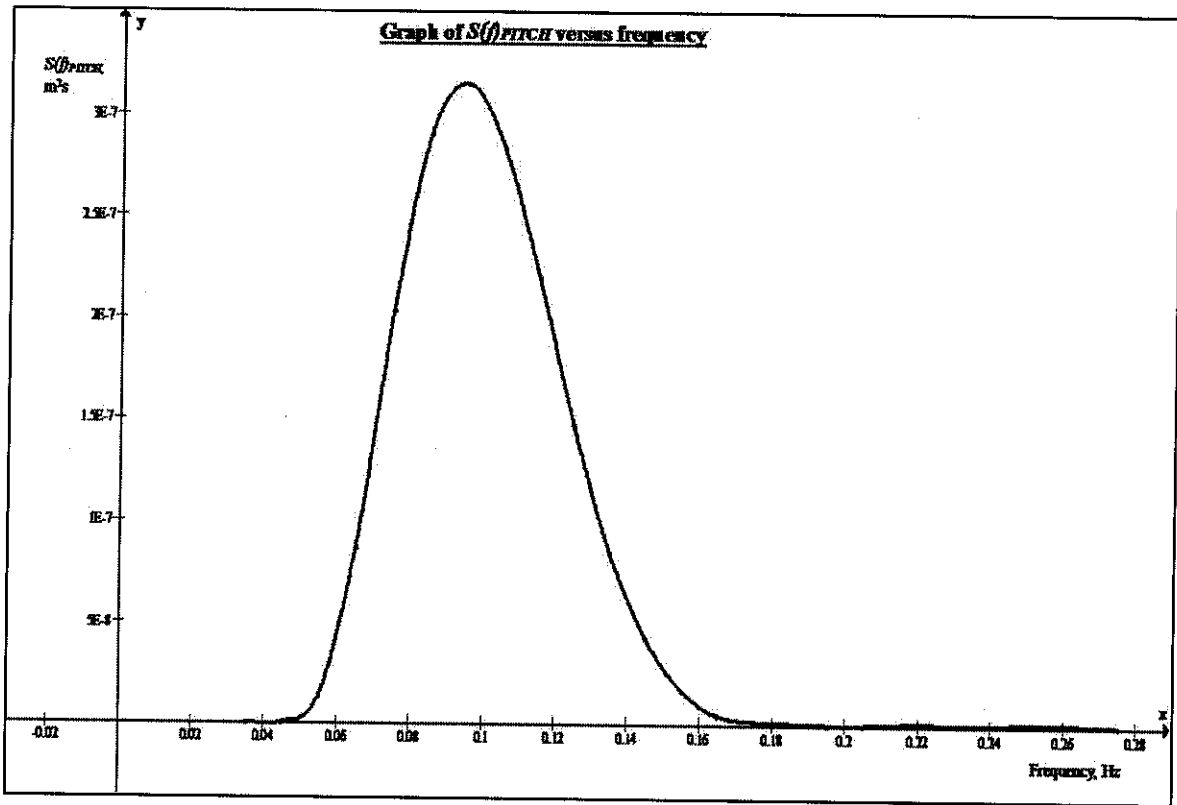


Figure 4.13: Graph of pitch spectrum,  $S(f)_{PITCH}$  versus frequency

Figure 4.13 shows pitch spectrum. The maximum peak value corresponding to the wave-spectral peaks, but also has additional peaks but very small. The peaks are subjected to the power of two of  $RAO_{PITCH}$  multiplied by  $S(f)$  in Equation (2.0). Area under the  $S(f)_{PITCH}$  was computed, giving a value of  $1.71 \times 10^{-8} m^2$ . The pitch responses versus series of time of 100s are plotted in Figure 4.14.

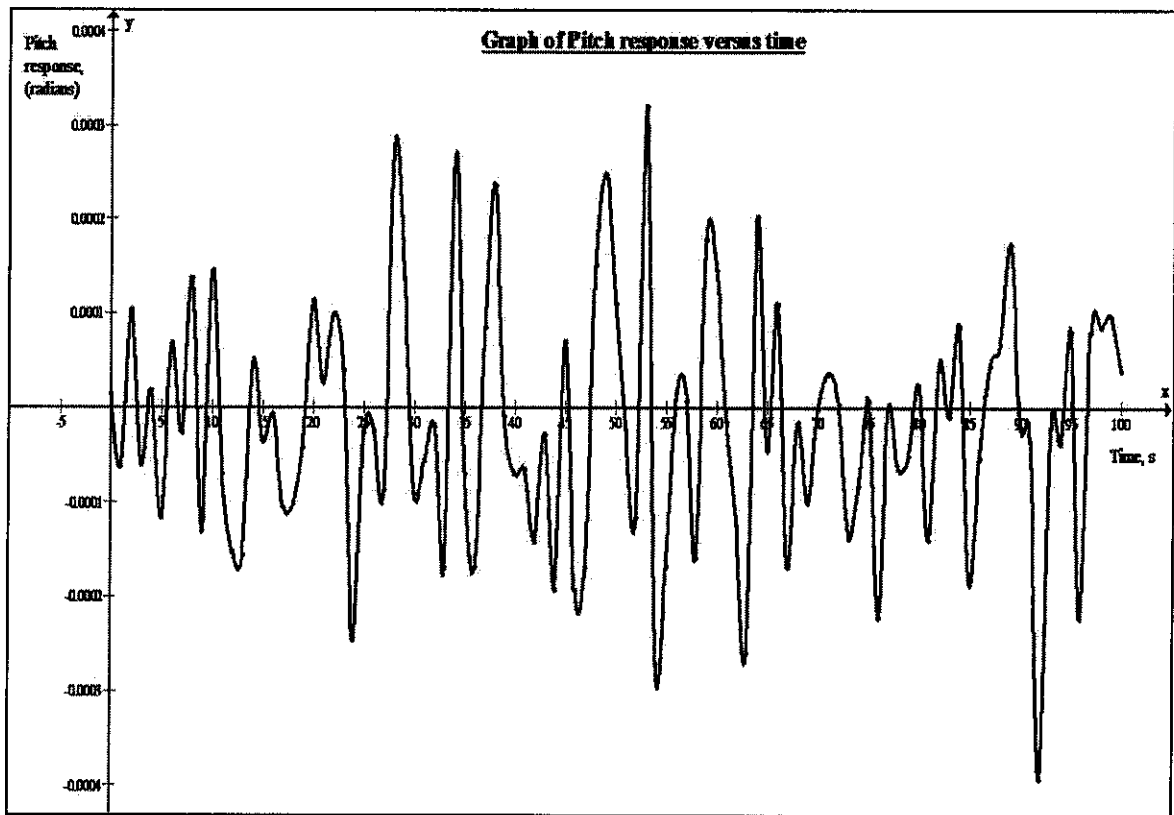


Figure 4.14: Graph of pitch response versus time

Positive pitch response indicates that the TLP is plunging forward at moment acting on z axis (unit in radian), induced by horizontal forces. Negative pitch response on the other hand indicates that the TLP is plunging backward at moment acting on z axis. Figure 4.14 shows the maximum positive pitch response gives value of 0.0003m at 53s while negative heave response gives value of 0.00039m at 92s.

## 4.8 Calculation of Responses by Varying Water Depth

Once the surge, heave and pitch analysis had been conducted, study was resumed by varying the water depth. A variation of 300m, 600m, 900m (original water depth), 1200m and 1500m were selected for the purpose. Different water depths were adopted in the responses calculation to examine the effect of water depth on the responses of TLP.

### 4.8.1 Effect of Water Depth on Surge

The surge response of TLP was recalculated by changing only the water depth and length of tethers. For example, for water depth of 300m, the length of tethers is 270m, because the water depth had to be deducted with the draught of 30m. Recalculation was done repeatedly with other water depth of 600m, 1200m, and 1500m, and the results are presented as graphs in Figure 4.15 and 4.16.

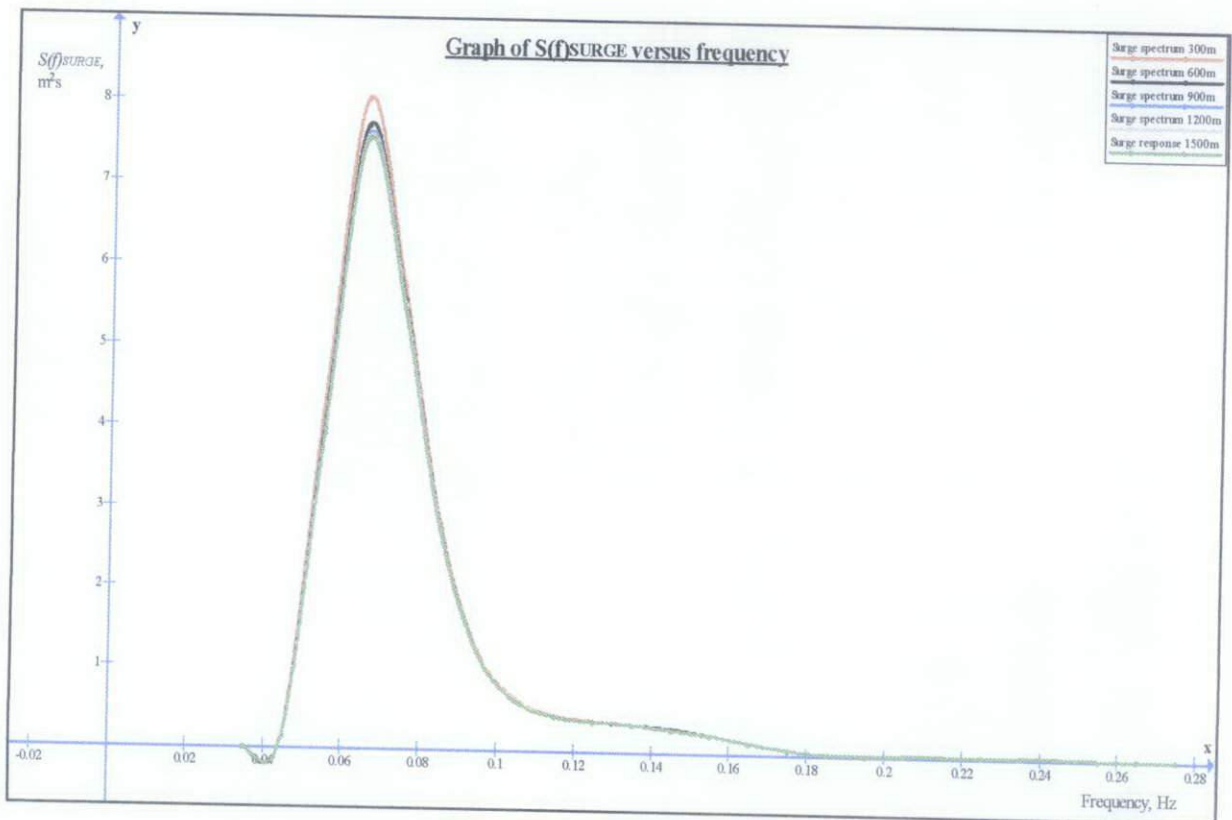


Figure 4.15: Graph of Surge Spectrum subjected to different water depths

Figure 4.15 presents the surge spectrum subjected to varying water depths. The graph shows that surge spectrum is affected by water depth, but slightly and the effect takes place at small range of frequency around 0.05-0.09Hz. The highest surge spectrum value lies in the water depth of 300m spectrum graph. For frequencies located outside of the 0.05-0.09Hz range, there is no effect on the surge spectrum.

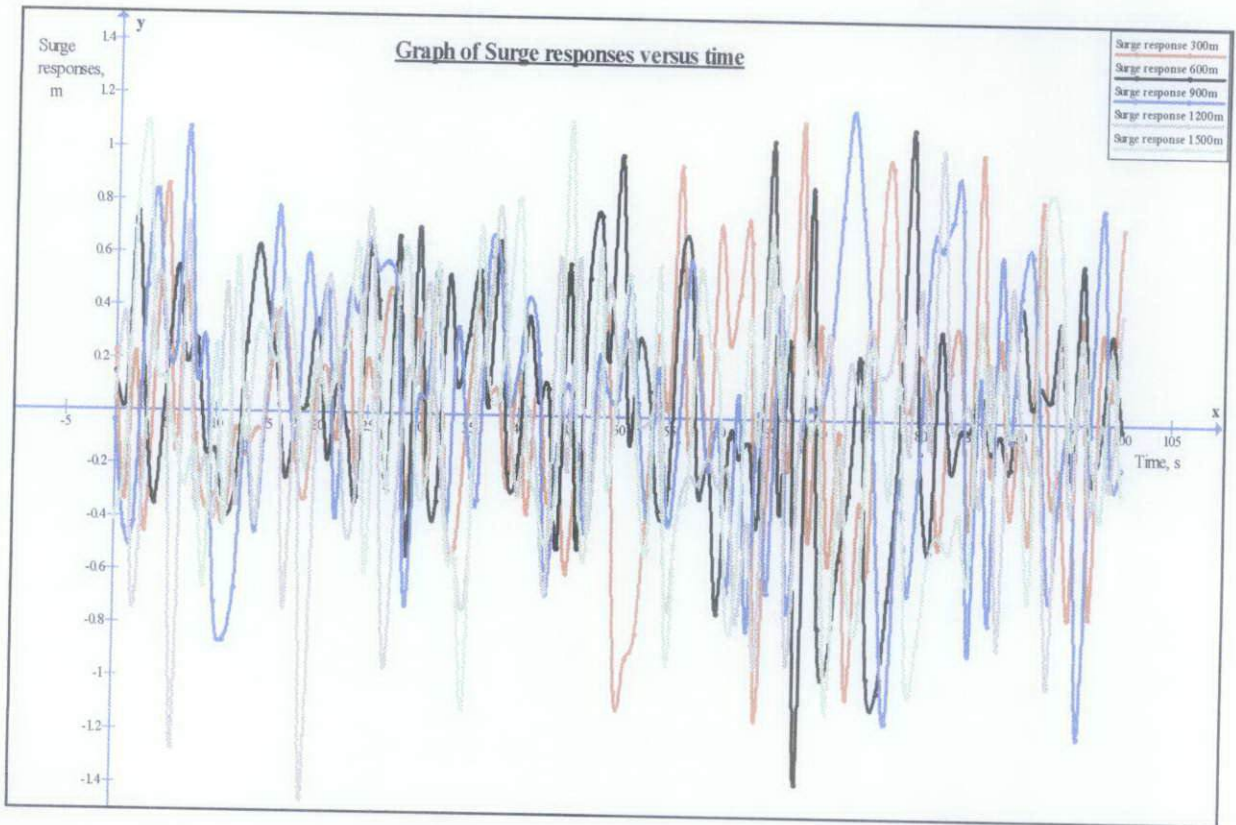


Figure 4.16: Graph of Surge Response subjected to different water depths

Figure 4.16 shows the surge responses subjected to varying water depths. The graph above shows the surge responses produced by different water depths, and the maximum surge response was 1.4m at water depth of 1200m. There is no apparent correlation between the responses and water depths since the responses are random.

#### 4.8.2 Effect of Water Depth on Heave

The heave response of TLP was recalculated by changing only the water depth. Recalculation was done repeatedly with other water depth of 300m, 600m, 1200m, and 1500m, and the results are shown as graphs in Figure 4.17 and 4.18.

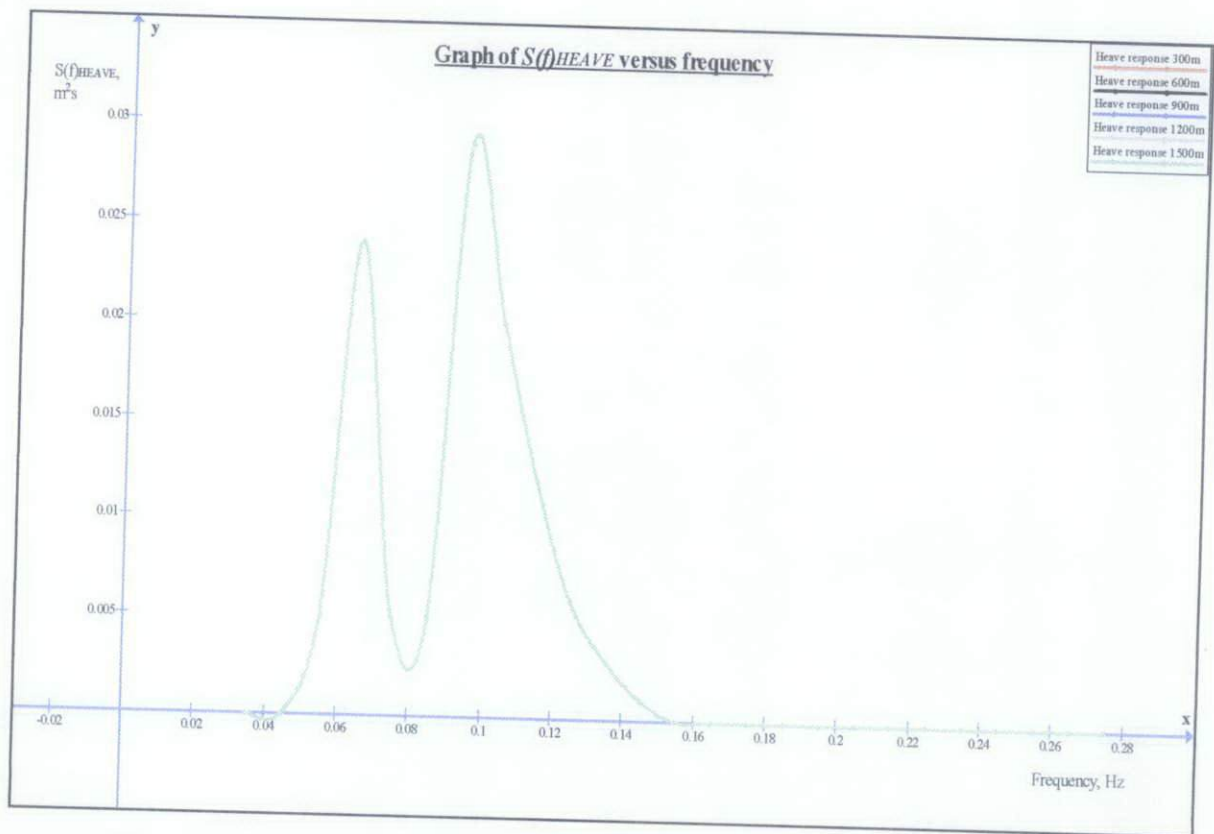


Figure 4.17: Graph of Heave Spectrum subjected to different water depths

Figure 4.17 above presents the heave spectrum subjected to varying water depths. The graph shows that heave spectrum is not affected by water depth. The spectrum produced for different water depths are same.

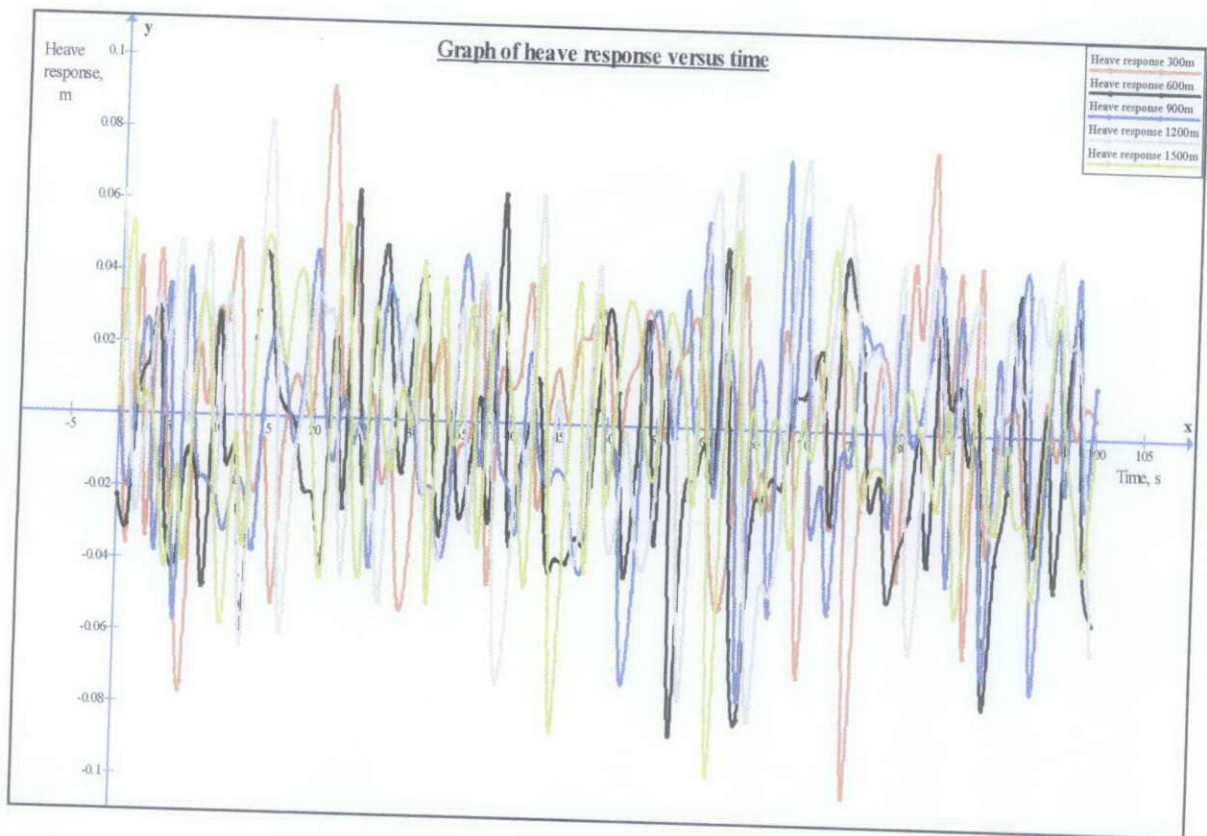


Figure 4.18: Graph of Heave Response subjected to different water depths

Heave responses produced by different water depths are shown in Figure 4.18. The maximum heave response was 0.1m at water depth of 300m. There is no apparent correlation between the responses and water depths since the responses are random.

### 4.8.3 Effect of Water Depth on Pitch

The pitch response of TLP was recalculated by changing only the water depth. Recalculation was done repeatedly with other water depth of 300m, 600m, 1200m, and 1500m, and the results are presented as graphs in Figure 4.19 and Figure 4.20.

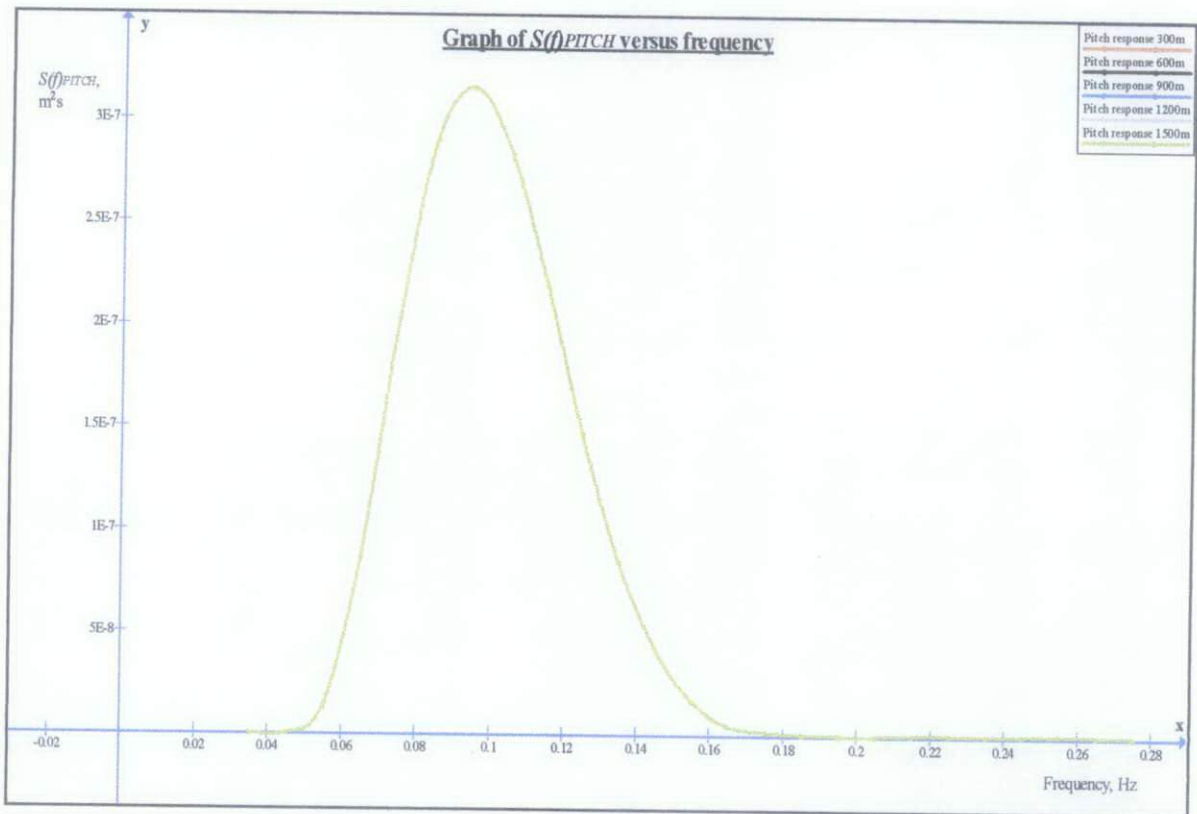


Figure 4.19: Graph of Pitch Spectrum subjected to different water depths

The graph in Figure 4.19 presents that pitch spectrum is not affected by water depth. The spectrum produced for different water depths are same.

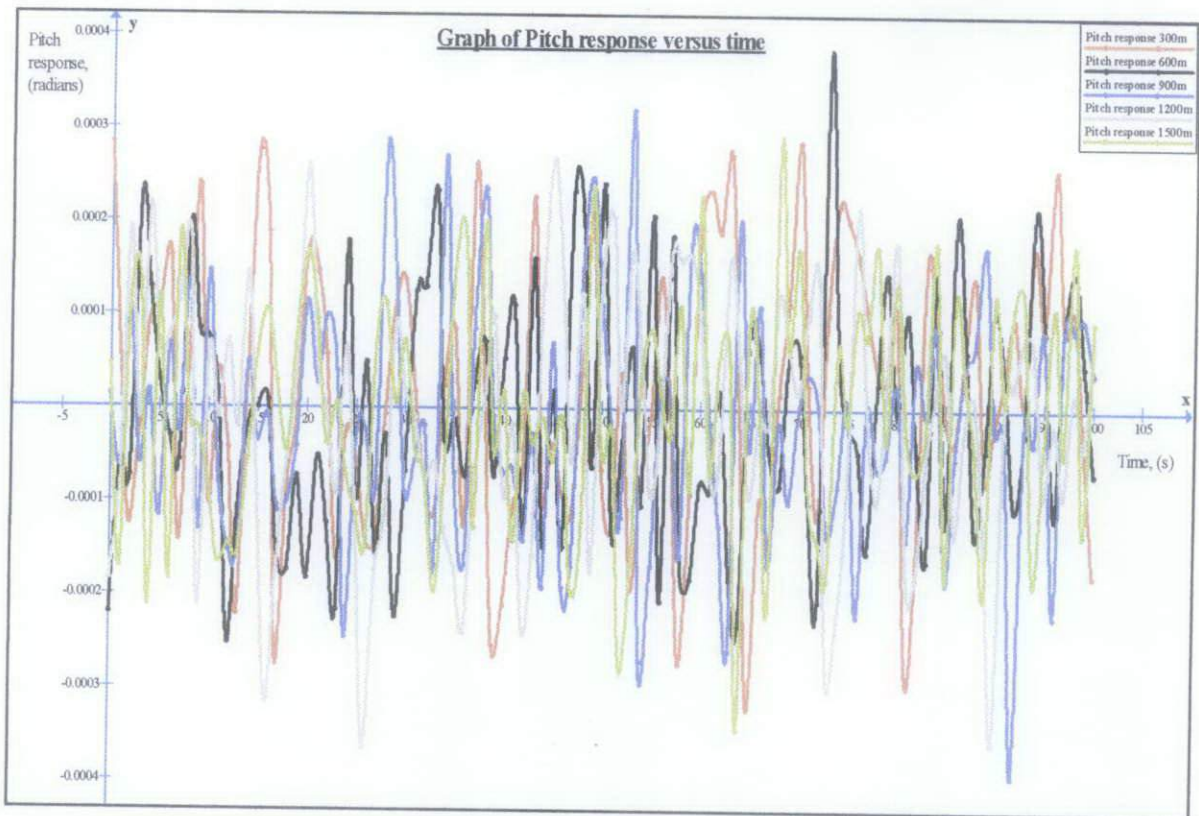


Figure 4.20: Graph of Pitch Response subjected to different water depths

Pitch responses produced by different water depths are presented in Figure 4.20. The maximum pitch response was 0.0004rad at water depth of 600m and 900m. There is no apparent correlation between the responses and water depths since the responses are random.

## CHAPTER 5

### *CONCLUSION AND RECOMMENDATIONS*

#### **5.0 Conclusion and Recommendations**

Analysis on the wave energy spectrum provides the amount of energy of the wave system. It was obtained by calculating the area under the spectrum graph. From the wave energy spectrum also, the wave time series can be obtained, by computing the water surface elevation subjected to time. Time series is used to predict the characteristics of wave, and crucial in designing procedure. Hull 1 and Hull 2 wave profile were not as same as Hull 3 because the x coordinates are different. The result of wave profile is depending on the value of x.

TLP is compliant in horizontal motion from the surge analysis. However, the surge responses were not so big. The highest response reached value of 1.4m. The surge response at Hull 1 and Hull 2 was not as the same as Hull 3, again because of the difference in the x value.

Heave analysis had been conducted and very small amount of motion been obtained. The maximum heave response was 0.1m which was very small compared to surge response.

This is because TLP is not complaint in vertical motion. Tendons which are tensile in normal condition prevent TLP from moving upward or downward.

Pitch analysis had been conducted and very small amount of pitch been obtained. The maximum pitch response was 0.0004rad which was very small. This is because TLP is not complaint in vertical motion. Tendons which are tensile in normal condition prevent TLP from move plunging forward or backward.

Based on the results of responses subjected to varying water depths, it is concluded that water depths do not affect behaviours of TLP. It is reasonable to state that the design of a TLP can be implemented at other water depths as well, as long as it is deep water. However, the case is restricted to only one parameter considered, which is water depth. Other important aspects, like bottom sea pressure, significant wave height, sea water conditions, current etc are not taken into account.

Thus, it is recommended that in the future, studies on other aspects should be conducted as well to analyze the parameters affecting TLP behaviour to improve the applicability of research. Studies may include real-life model of TLP and laboratory tests to compare theoretical results with the experimental results done by tests in the laboratory.

## REFERENCES

- [1] Kurian, V.J. (2008) *Chapter 1: General Introduction*. Malaysia: University Technology Petronas. 50-page notes on the introduction of offshore structures, accessed on 21<sup>st</sup> July 2008 in Lecture 1 for VAB 4423 "Design of Offshore Structure".
  
- [2] Chakrabarti, S. K., (2005) *Handbook of Offshore Engineering*. ELSEVIER Ltd.
  
- [3] U.S. Department of the Interior, (2004) *Minerals Management Service*. Gulf of Mexico OCS Region.
  
- [4] Tihardy John, (2003) *Climate Change: Causes, Effects, and Solutions*. Chichester, England: John Wiley & Sons Ltd.
  
- [5] Macdonald, Glen M., (2003) *Biogeography, Introduction to Space, Time and Life*. John Wiley & Sons, Inc

- [6] Chakrabarti, S.K., (2001) *Hydrodynamics of Structures*. WIT Press.
- [7] Anonymous. (2008) *Shell in the US*. [Online] Available from: URL <http://www.shell.us> [Accessed on 18<sup>th</sup> February 2008]
- [8] Anonymous. (2008) *Development Options with SeaStar TLPs* [Online] Available from: URL <http://www.atlantia.com/seastar/> [Accessed on 4<sup>th</sup> August 2008]
- [9] Anonymous. (2008) *Brutus : Fact Sheet*. [Online] Available from: URL <http://www.theoildrum.com/files/Brutus%20Fact%20Sheet.pdf> [Accessed on 31<sup>st</sup> March 2008]
- [10] Anonymous. (2008) *Current local weather, radar and forecasts from the Weather Channel*. [Online] Available from: URL <http://www.weather.com> [Accessed on 25<sup>th</sup> February 2008]
- [11] Chandrasekaran, S., Jain, A.K., (2000) *Dynamic behaviour of square and triangular offshore tension leg platforms under regular wave loads*. Indian Institute of Technology.
- [12] Kurian, V.J., Idichandy, V.G., and Ganapathy, C., (1993) *Hydrodynamics response of tension-leg platform- a model*. Indian Institute of Technology.

## **APPENDIX A**

### **SURGE PARAMETERS**

**(For water depth of 300m, 600m, 900m, 1200m and 1500m)**

$H_s = 7.5$  m  
 $\alpha = 0.0081$   
 $\omega_o = 0.4588$  rad/sec  
 $f_o = 0.0730$  Hz  
 $K_{SURGE} = 507284.5623$  N/m  
 $M_{SURGE} = 78501330$  kg  
 $C = 1262102$  kg/m

f(l) (Hz)	T (s)	$\omega$ (rad/s)	S(f) (m <sup>2</sup> s)	H(f) (m)	H(f) <sub>SURGE</sub> (m)	F (kN)	L (m)	K (N/m)	RAO <sub>SURGE</sub>	RAO <sub>SURGE</sub> <sup>2</sup>	S(f) <sub>SURGE</sub> (m <sup>2</sup> s)
0.035	28.571	0.220	0.00	0.000	0.000	0.215	1274	507285	0.647	0.418	0.000
0.045	22.222	0.283	0.5	0.194	0.107	309.545	771	507285	0.552	0.304	0.143
0.055	18.182	0.346	20.5	1.281	0.585	2596.888	516	507285	0.457	0.208	4.278
0.065	15.385	0.408	59.0	2.172	0.801	5043.696	369	507285	0.369	0.136	8.016
0.075	13.333	0.471	68.6	2.343	0.678	5737.049	277	507285	0.289	0.084	5.738
0.085	11.765	0.534	57.1	2.137	0.474	5191.023	216	507285	0.222	0.049	2.811
0.095	10.526	0.597	41.8	1.828	0.315	4322.544	173	507285	0.172	0.030	1.238
0.105	9.524	0.660	29.2	1.530	0.223	3757.076	142	507285	0.146	0.021	0.623
0.115	8.696	0.723	20.3	1.274	0.185	3736.394	118	507285	0.145	0.021	0.426
0.125	8.000	0.785	14.2	1.064	0.171	4100.973	100	507285	0.161	0.026	0.366
0.135	7.407	0.848	10.0	0.895	0.162	4546.043	86	507285	0.181	0.033	0.330
0.145	6.897	0.911	7.2	0.759	0.149	4821.484	74	507285	0.197	0.039	0.278
0.155	6.452	0.974	5.3	0.648	0.128	4746.951	65	507285	0.198	0.039	0.206
0.165	6.061	1.037	3.9	0.558	0.100	4209.838	57	507285	0.180	0.032	0.126
0.175	5.714	1.100	2.9	0.484	0.068	3195.340	51	507285	0.140	0.020	0.057
0.185	5.405	1.162	2.2	0.423	0.034	1814.534	46	507285	0.081	0.007	0.015
0.195	5.128	1.225	1.7	0.372	0.005	306.410	41	507285	0.014	0.000	0.000
0.205	4.878	1.288	1.4	0.329	0.016	1018.163	37	507285	0.048	0.002	0.003
0.215	4.651	1.351	1.1	0.293	0.026	1870.756	34	507285	0.090	0.008	0.009
0.225	4.444	1.414	0.9	0.262	0.027	2099.696	31	507285	0.103	0.011	0.009
0.235	4.255	1.477	0.7	0.235	0.021	1761.449	28	507285	0.088	0.008	0.005
0.245	4.082	1.539	0.6	0.212	0.012	1110.027	26	507285	0.056	0.003	0.002
0.255	3.922	1.602	0.5	0.192	0.005	478.450	24	507285	0.025	0.001	0.000
0.265	3.774	1.665	0.4	0.174	0.001	104.564	22	507285	0.006	0.000	0.000
0.275	3.636	1.728	0.3	0.159	0.000	3.526	21	507285	0.000	0.000	0.000

Surge calculation at water depth 600m

$$\begin{aligned}
 H_s &= 7.5 \text{ m} & K_{\text{SURGE}} &= 240292.69 \text{ N/m} \\
 \alpha &= 0.0081 & M_{\text{SURGE}} &= 78501330 \text{ kg} \\
 \omega_0 &= 0.4588 \text{ rad/sec} & C &= 868638 \text{ kg/m} \\
 f_0 &= 0.0730 \text{ Hz}
 \end{aligned}$$

f(1) (Hz)	T (s)	$\omega$ (rad/s)	S(f) (m <sup>2</sup> s)	H(f) (m)	H(f) <sub>SURGE</sub> (m)	F (kN)	L (m)	K (N/m)	RAO <sub>SURGE</sub>	RAO <sub>SURGE</sub> <sup>2</sup>	S(f) <sub>SURGE</sub> (m <sup>2</sup> s)
0.035	28.571	0.220	0.00	0.000	0.000	0.215	1274	240293	0.599	0.359	0.000
0.045	22.222	0.283	0.5	0.194	0.102	309.545	771	240293	0.528	0.279	0.131
0.055	18.182	0.346	20.5	1.281	0.568	2596.888	516	240293	0.443	0.197	4.037
0.065	15.385	0.408	59.0	2.172	0.785	5043.696	369	240293	0.361	0.130	7.693
0.075	13.333	0.471	68.6	2.343	0.667	5737.049	277	240293	0.285	0.081	5.565
0.085	11.765	0.534	57.1	2.137	0.469	5191.023	216	240293	0.219	0.048	2.745
0.095	10.526	0.597	41.8	1.828	0.312	4322.544	173	240293	0.171	0.029	1.215
0.105	9.524	0.660	29.2	1.530	0.221	3757.076	142	240293	0.145	0.021	0.613
0.115	8.696	0.723	20.3	1.274	0.183	3736.394	118	240293	0.144	0.021	0.420
0.125	8.000	0.785	14.2	1.064	0.170	4100.973	100	240293	0.160	0.026	0.362
0.135	7.407	0.848	10.0	0.895	0.162	4546.043	86	240293	0.181	0.033	0.327
0.145	6.897	0.911	7.2	0.759	0.149	4821.484	74	240293	0.196	0.038	0.276
0.155	6.452	0.974	5.3	0.648	0.128	4746.951	65	240293	0.197	0.039	0.205
0.165	6.061	1.037	3.9	0.558	0.100	4209.838	57	240293	0.179	0.032	0.125
0.175	5.714	1.100	2.9	0.484	0.068	3195.340	51	240293	0.139	0.019	0.057
0.185	5.405	1.162	2.2	0.423	0.034	1814.534	46	240293	0.081	0.007	0.015
0.195	5.128	1.225	1.7	0.372	0.005	306.410	41	240293	0.014	0.000	0.000
0.205	4.878	1.288	1.4	0.329	0.016	1018.163	37	240293	0.048	0.002	0.003
0.215	4.651	1.351	1.1	0.293	0.026	1870.756	34	240293	0.089	0.008	0.009
0.225	4.444	1.414	0.9	0.262	0.027	2099.696	31	240293	0.103	0.011	0.009
0.235	4.255	1.477	0.7	0.235	0.021	1761.449	28	240293	0.088	0.008	0.005
0.245	4.082	1.539	0.6	0.212	0.012	1110.027	26	240293	0.056	0.003	0.002
0.255	3.922	1.602	0.5	0.192	0.005	478.450	24	240293	0.025	0.001	0.000
0.265	3.774	1.665	0.4	0.174	0.001	104.564	22	240293	0.006	0.000	0.000
0.275	3.636	1.728	0.3	0.159	0.000	3.526	21	240293	0.000	0.000	0.000

Surge calculation at water depth 900m

$H_s = 7.5$  m  
 $\alpha = 0.0081$   
 $\omega_0 = 0.4588$  rad/sec  
 $f_0 = 0.0730$  Hz

$K_{SURGE} = 157433.14$  N/m  
 $M_{SURGE} = 78501330$  kg  
 $C = 703099$  kg/m

f(1) (Hz)	T (s)	$\omega$ (rad/s)	S(f) (m <sup>2</sup> s)	H(f) (m)	H(f) <sub>SURGE</sub> (m)	F (kN)	L (m)	K (N/m)	RAO <sub>SURGE</sub>	RAO <sub>SURGE</sub> <sup>2</sup>	S(f) <sub>SURGE</sub> (m <sup>2</sup> s)
0.035	28.571	0.220	0.00	0.000	0.000	0.220	1274	157433	0.601	0.361	0.000
0.045	22.222	0.283	0.5	0.194	0.101	309.545	771	157433	0.521	0.271	0.128
0.055	18.182	0.346	20.5	1.281	0.563	2596.888	516	157433	0.440	0.193	3.966
0.065	15.385	0.408	59.0	2.172	0.780	5043.696	369	157433	0.359	0.129	7.597
0.075	13.333	0.471	68.6	2.343	0.664	5737.049	277	157433	0.283	0.080	5.513
0.085	11.765	0.534	57.1	2.137	0.467	5191.023	216	157433	0.219	0.048	2.725
0.095	10.526	0.597	41.8	1.828	0.311	4322.544	173	157433	0.170	0.029	1.207
0.105	9.524	0.660	29.2	1.530	0.221	3757.076	142	157433	0.144	0.021	0.610
0.115	8.696	0.723	20.3	1.274	0.183	3736.394	118	157433	0.144	0.021	0.419
0.125	8.000	0.785	14.2	1.064	0.170	4100.973	100	157433	0.160	0.025	0.361
0.135	7.407	0.848	10.0	0.895	0.161	4546.043	86	157433	0.180	0.033	0.326
0.145	6.897	0.911	7.2	0.759	0.148	4821.484	74	157433	0.196	0.038	0.275
0.155	6.452	0.974	5.3	0.648	0.128	4746.951	65	157433	0.197	0.039	0.204
0.165	6.061	1.037	3.9	0.558	0.100	4209.838	57	157433	0.179	0.032	0.125
0.175	5.714	1.100	2.9	0.484	0.067	3195.340	51	157433	0.139	0.019	0.057
0.185	5.405	1.162	2.2	0.423	0.034	1814.534	46	157433	0.081	0.007	0.015
0.195	5.128	1.225	1.7	0.372	0.005	306.410	41	157433	0.014	0.000	0.000
0.205	4.878	1.288	1.4	0.329	0.016	1018.163	37	157433	0.048	0.002	0.003
0.215	4.651	1.351	1.1	0.293	0.026	1870.756	34	157433	0.089	0.008	0.009
0.225	4.444	1.414	0.9	0.262	0.027	2099.696	31	157433	0.102	0.010	0.009
0.235	4.255	1.477	0.7	0.235	0.021	1761.449	28	157433	0.088	0.008	0.005
0.245	4.082	1.539	0.6	0.212	0.012	1110.027	26	157433	0.056	0.003	0.002
0.255	3.922	1.602	0.5	0.192	0.005	478.450	24	157433	0.025	0.001	0.000
0.265	3.774	1.665	0.4	0.174	0.001	104.564	22	157433	0.006	0.000	0.000
0.275	3.636	1.728	0.3	0.159	0.000	3.526	21	157433	0.000	0.000	0.000

Surge calculation at water depth 1200m

$H_s = 7.5$  m  
 $\alpha = 0.0081$   
 $\omega_0 = 0.4588$  rad/sec  
 $f_0 = 0.0730$  Hz  
 $K_{SURGE} = 117065.668$  N/m  
 $M_{SURGE} = 78501330$  kg  
 $C = 606294$  kg/m

f(1) (Hz)	T (s)	$\omega$ (rad/s)	S(f) (m <sup>2</sup> s)	H(f) (m)	H(f) <sub>SURGE</sub> (m)	F (kN)	L (m)	K (N/m)	RAO <sub>SURGE</sub>	RAO <sub>SURGE</sub> <sup>2</sup>	S(f) <sub>SURGE</sub> (m <sup>2</sup> s)
0.035	28.571	0.220	0.00	0.000	0.000	0.220	1274	117066	0.594	0.353	0.000
0.045	22.222	0.283	0.5	0.194	0.100	309.559	771	117066	0.518	0.268	0.126
0.055	18.182	0.346	20.5	1.281	0.561	2596.890	516	117066	0.438	0.192	3.932
0.065	15.385	0.408	59.0	2.172	0.777	5043.696	369	117066	0.358	0.128	7.551
0.075	13.333	0.471	68.6	2.343	0.663	5737.049	277	117066	0.283	0.080	5.487
0.085	11.765	0.534	57.1	2.137	0.466	5191.023	216	117066	0.218	0.048	2.715
0.095	10.526	0.597	41.8	1.828	0.310	4322.544	173	117066	0.170	0.029	1.204
0.105	9.524	0.660	29.2	1.530	0.221	3757.076	142	117066	0.144	0.021	0.609
0.115	8.696	0.723	20.3	1.274	0.183	3736.394	118	117066	0.144	0.021	0.418
0.125	8.000	0.785	14.2	1.064	0.170	4100.973	100	117066	0.160	0.025	0.360
0.135	7.407	0.848	10.0	0.895	0.161	4546.043	86	117066	0.180	0.032	0.325
0.145	6.897	0.911	7.2	0.759	0.148	4821.484	74	117066	0.195	0.038	0.275
0.155	6.452	0.974	5.3	0.648	0.128	4746.951	65	117066	0.197	0.039	0.204
0.165	6.061	1.037	3.9	0.558	0.100	4209.838	57	117066	0.179	0.032	0.125
0.175	5.714	1.100	2.9	0.484	0.067	3195.340	51	117066	0.139	0.019	0.057
0.185	5.405	1.162	2.2	0.423	0.034	1814.534	46	117066	0.081	0.007	0.015
0.195	5.128	1.225	1.7	0.372	0.005	306.410	41	117066	0.014	0.000	0.000
0.205	4.878	1.288	1.4	0.329	0.016	1018.163	37	117066	0.048	0.002	0.003
0.215	4.651	1.351	1.1	0.293	0.026	1870.756	34	117066	0.089	0.008	0.009
0.225	4.444	1.414	0.9	0.262	0.027	2099.696	31	117066	0.102	0.010	0.009
0.235	4.255	1.477	0.7	0.235	0.021	1761.449	28	117066	0.088	0.008	0.005
0.245	4.082	1.539	0.6	0.212	0.012	1110.027	26	117066	0.056	0.003	0.002
0.255	3.922	1.602	0.5	0.192	0.005	478.450	24	117066	0.025	0.001	0.000
0.265	3.774	1.665	0.4	0.174	0.001	104.564	22	117066	0.006	0.000	0.000
0.275	3.636	1.728	0.3	0.159	0.000	3.526	21	117066	0.000	0.000	0.000

Surge calculation at water depth 1500m

$H_s = 7.5$  m  
 $\alpha = 0.0081$   
 $\omega_0 = 0.4588$  rad/sec  
 $f_0 = 0.0730$  Hz  
 $K_{SURGE} = 93174.71553$  N/m  
 $M_{SURGE} = 78501330$  kg  
 $C = 540901$  kg/m

f(l) (Hz)	T (s)	$\omega$ (rad/s)	S(f) (m <sup>2</sup> s)	H(f) (m)	H(f) <sub>SURGE</sub> (m)	F (kN)	L (m)	K (N/m)	RAO <sub>SURGE</sub>	RAO <sub>SURGE</sub> <sup>2</sup>	S(f) <sub>SURGE</sub> (m <sup>2</sup> s)
0.035	28.571	0.220	0.00	0.000	0.000	0.220	1274	93175	0.591	0.349	0.000
0.045	22.222	0.283	0.5	0.194	0.100	309.559	771	93175	0.516	0.266	0.125
0.055	18.182	0.346	20.5	1.281	0.559	2596.890	516	93175	0.437	0.191	3.912
0.065	15.385	0.408	59.0	2.172	0.776	5043.696	369	93175	0.357	0.128	7.523
0.075	13.333	0.471	68.6	2.343	0.662	5737.049	277	93175	0.282	0.080	5.473
0.085	11.765	0.534	57.1	2.137	0.466	5191.023	216	93175	0.218	0.047	2.709
0.095	10.526	0.597	41.8	1.828	0.310	4322.544	173	93175	0.170	0.029	1.202
0.105	9.524	0.660	29.2	1.530	0.221	3757.076	142	93175	0.144	0.021	0.608
0.115	8.696	0.723	20.3	1.274	0.183	3736.394	118	93175	0.143	0.021	0.417
0.125	8.000	0.785	14.2	1.064	0.170	4100.973	100	93175	0.159	0.025	0.360
0.135	7.407	0.848	10.0	0.895	0.161	4546.043	86	93175	0.180	0.032	0.325
0.145	6.897	0.911	7.2	0.759	0.148	4821.484	74	93175	0.195	0.038	0.275
0.155	6.452	0.974	5.3	0.648	0.128	4746.951	65	93175	0.197	0.039	0.204
0.165	6.061	1.037	3.9	0.558	0.100	4209.838	57	93175	0.179	0.032	0.125
0.175	5.714	1.100	2.9	0.484	0.067	3195.340	51	93175	0.139	0.019	0.057
0.185	5.405	1.162	2.2	0.423	0.034	1814.534	46	93175	0.081	0.007	0.015
0.195	5.128	1.225	1.7	0.372	0.005	306.410	41	93175	0.014	0.000	0.000
0.205	4.878	1.288	1.4	0.329	0.016	1018.163	37	93175	0.048	0.002	0.003
0.215	4.651	1.351	1.1	0.293	0.026	1870.756	34	93175	0.089	0.008	0.009
0.225	4.444	1.414	0.9	0.262	0.027	2099.696	31	93175	0.102	0.010	0.009
0.235	4.255	1.477	0.7	0.235	0.021	1761.449	28	93175	0.088	0.008	0.005
0.245	4.082	1.539	0.6	0.212	0.012	1110.027	26	93175	0.056	0.003	0.002
0.255	3.922	1.602	0.5	0.192	0.005	478.450	24	93175	0.025	0.001	0.000
0.265	3.774	1.665	0.4	0.174	0.001	104.564	22	93175	0.006	0.000	0.000
0.275	3.636	1.728	0.3	0.159	0.000	3.526	21	93175	0.000	0.000	0.000

## **APPENDIX B**

### **HEAVE PARAMETERS**

**(For water depth of 900m)**

Heave calculation at water depth 900m

$H_s = 7.5 \text{ m}$   
 $\alpha = 0.0081$   
 $\omega_0 = 0.4588 \text{ rad/sec}$   
 $f_0 = 0.0730 \text{ Hz}$

$K_{HEAVE} = 315523078 \text{ N/m}$   
 $M_{HEAVE} = 76214085 \text{ kg}$   
 $C = 98076098 \text{ kg/m}$

$f(1) \text{ (Hz)}$	$T \text{ (s)}$	$\omega \text{ (rad/s)}$	$S(f) \text{ (m}^2\text{s)}$	$H(f) \text{ (m)}$	$H(f)_{HEAVE} \text{ (m)}$	$F \text{ (kN)}$	$L \text{ (m)}$	$K \text{ (N/m)}$	$RAO_{HEAVE}$	$RAO_{HEAVE}^2$	$S(f)_{HEAVE} \text{ (m}^2\text{s)}$
0.035	28.571	0.220	0.00	0.000	0.000000	0.20	1274	315523000	0.000006	0.0000000000	0.0000000000
0.045	22.222	0.283	0.5	0.194	0.000002	353.12	771	315523000	0.000012	0.0000000001	0.0000000001
0.055	18.182	0.346	20.5	1.281	0.000020	3148.23	516	315523000	0.000016	0.0000000003	0.0000000003
0.065	15.385	0.408	59.0	2.172	0.000043	6590.46	369	315523000	0.000020	0.0000000004	0.0000000004
0.075	13.333	0.471	68.6	2.343	0.000020	3075.69	277	315523000	0.000009	0.0000000001	0.0000000001
0.085	11.765	0.534	57.1	2.137	0.000019	2895.61	216	315523000	0.000009	0.0000000001	0.0000000001
0.095	10.526	0.597	41.8	1.828	0.000048	6990.11	173	315523000	0.000026	0.0000000007	0.0000000007
0.105	9.524	0.660	29.2	1.530	0.000039	5617.25	142	315523000	0.000025	0.0000000006	0.0000000006
0.115	8.696	0.723	20.3	1.274	0.000030	4238.46	118	315523000	0.000023	0.0000000005	0.0000000005
0.125	8.000	0.785	14.2	1.064	0.000022	3015.22	100	315523000	0.000020	0.0000000004	0.0000000004
0.135	7.407	0.848	10.0	0.895	0.000015	2016.28	86	315523000	0.000016	0.0000000003	0.0000000003
0.145	6.897	0.911	7.2	0.759	0.000009	1258.68	74	315523000	0.000012	0.0000000002	0.0000000002
0.155	6.452	0.974	5.3	0.648	0.000006	732.46	65	315523000	0.000009	0.0000000001	0.0000000001
0.165	6.061	1.037	3.9	0.558	0.000003	368.27	57	315523000	0.000005	0.0000000000	0.0000000000
0.175	5.714	1.100	2.9	0.484	0.000002	220.67	51	315523000	0.000004	0.0000000000	0.0000000000
0.185	5.405	1.162	2.2	0.423	0.000001	171.30	46	315523000	0.000003	0.0000000000	0.0000000000
0.195	5.128	1.225	1.7	0.372	0.000001	139.68	41	315523000	0.000003	0.0000000000	0.0000000000
0.205	4.878	1.288	1.4	0.329	0.000001	106.70	37	315523000	0.000003	0.0000000000	0.0000000000
0.215	4.651	1.351	1.1	0.293	0.000001	74.99	34	315523000	0.000002	0.0000000000	0.0000000000
0.225	4.444	1.414	0.9	0.262	0.000000	48.51	31	315523000	0.000002	0.0000000000	0.0000000000
0.235	4.255	1.477	0.7	0.235	0.000000	28.83	28	315523000	0.000001	0.0000000000	0.0000000000
0.245	4.082	1.539	0.6	0.212	0.000000	15.64	26	315523000	0.000001	0.0000000000	0.0000000000
0.255	3.922	1.602	0.5	0.192	0.000000	10.44	24	315523000	0.000001	0.0000000000	0.0000000000
0.265	3.774	1.665	0.4	0.174	0.000000	3.37	22	315523000	0.000000	0.0000000000	0.0000000000
0.275	3.636	1.728	0.3	0.159	0.000000	4.66	21	315523000	0.000000	0.0000000000	0.0000000000

## **APPENDIX C**

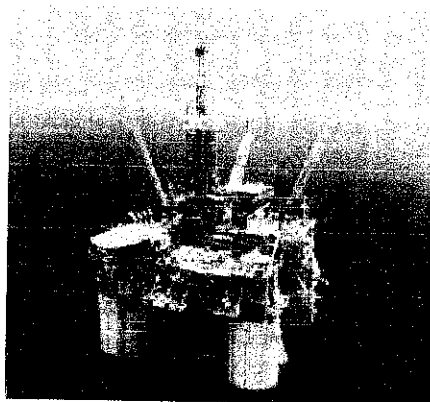
### **PITCH PARAMETERS**

**(For water depth of 900m)**

Pitch calculation of water depth 900m

$H_s = 7.5$  m  
 $\alpha = 0.0081$   
 $\omega_0 = 0.4588$  rad/sec  
 $f_0 = 0.0730$  Hz  
 $\omega_{\text{PITCH}} = 3.1416$  rad/sec, with  $T_{\text{PITCH}} = 2$ s  
 $K_{\text{PITCH}} = 1265186243284$  Nm / rad  
 $M_{\text{PITCH}} = 128190167698$  kg m<sup>2</sup>  
 $C = 8054425782$  kg m<sup>2</sup> / s (rad<sup>1/2</sup>)

f(1) (Hz)	T (s)	$\omega$ (rad/s)	S(f) (m <sup>2</sup> s)	H(f) (m)	H(f) <sub>PITCH</sub> (m)	F (Nm)	L (m)	K (Nm/rad)	RAO <sub>PITCH</sub>	RAO <sub>PITCH</sub> <sup>2</sup>	S(f) <sub>PITCH</sub> (m <sup>2</sup> s)
0.035	28.6	0.220	0.00	0.000	0.000000	0.971	1274	1265186243284	0.000008	0.000000001	0.000000000
0.045	22.2	0.283	0.5	0.194	0.000029	1794.754	771	1265186243284	0.000015	0.000000002	0.000000000
0.055	18.2	0.346	20.5	1.281	0.000319	19951.372	516	1265186243284	0.000025	0.000000006	0.000000001
0.065	15.4	0.408	59.0	2.172	0.000833	51803.436	369	1265186243284	0.000038	0.000000015	0.000000009
0.075	13.3	0.471	68.6	2.343	0.001274	78772.299	277	1265186243284	0.000054	0.000000030	0.000000020
0.085	11.8	0.534	57.1	2.137	0.001524	93622.122	216	1265186243284	0.000071	0.000000051	0.000000029
0.095	10.5	0.597	41.8	1.828	0.001588	96828.941	173	1265186243284	0.000087	0.000000075	0.000000032
0.105	9.5	0.660	29.2	1.530	0.001506	91063.380	142	1265186243284	0.000098	0.000000097	0.000000028
0.115	8.7	0.723	20.3	1.274	0.001323	79282.859	118	1265186243284	0.000104	0.000000108	0.000000022
0.125	8.0	0.785	14.2	1.064	0.001083	64251.538	100	1265186243284	0.000102	0.000000104	0.000000015
0.135	7.4	0.848	10.0	0.895	0.000825	48376.782	86	1265186243284	0.000092	0.000000085	0.000000009
0.145	6.9	0.911	7.2	0.759	0.000582	33718.259	74	1265186243284	0.000077	0.000000059	0.000000004
0.155	6.5	0.974	5.3	0.648	0.000366	20948.024	65	1265186243284	0.000057	0.000000032	0.000000002
0.165	6.1	1.037	3.9	0.558	0.000193	10898.606	57	1265186243284	0.000035	0.000000012	0.000000000
0.175	5.7	1.100	2.9	0.484	0.000105	5814.770	51	1265186243284	0.000022	0.000000005	0.000000000
0.185	5.4	1.162	2.2	0.423	0.000046	2526.867	46	1265186243284	0.000011	0.000000001	0.000000000
0.195	5.1	1.225	1.7	0.372	0.000020	1095.673	41	1265186243284	0.000005	0.000000000	0.000000000
0.205	4.9	1.288	1.4	0.329	0.000011	-572.235	37	1265186243284	-0.000003	0.000000000	0.000000000
0.215	4.7	1.351	1.1	0.293	0.0000047	-2398.444	34	1265186243284	-0.000016	0.000000003	0.000000000
0.225	4.4	1.414	0.9	0.262	0.0000069	-3473.578	31	1265186243284	-0.000026	0.000000007	0.000000000
0.235	4.3	1.477	0.7	0.235	0.0000068	-3340.619	28	1265186243284	-0.000029	0.000000008	0.000000000
0.245	4.1	1.539	0.6	0.212	0.0000066	-3176.709	26	1265186243284	-0.000031	0.000000010	0.000000000
0.255	3.9	1.602	0.5	0.192	0.0000077	-3615.944	24	1265186243284	-0.000040	0.000000016	0.000000000
0.265	3.8	1.665	0.4	0.174	0.0000061	-2763.741	22	1265186243284	-0.000035	0.000000012	0.000000000
0.275	3.6	1.728	0.3	0.159	0.0000015	-667.484	21	1265186243284	-0.000010	0.000000001	0.000000000



BRUTUS

## FACT SHEET

### EXPLORATION AND DISCOVERY

- Brutus encompasses two OCS leases in the Green Canyon area – Blocks 158 and 202. It is located approximately 165 miles southwest of New Orleans in water depths ranging from 2,750 to 3,300 feet.
- The leases were acquired in OCS Lease Sale 98 in March 1985, for a total bonus of \$ 15.5 million.
- Shell Offshore Inc. owns 100% of the leases.
- The discovery well was drilled on Green Canyon Block 158 in December 1988. An appraisal well was drilled on Green Canyon Block 158 in 1994. A third well was drilled in 1997 on that same block, with a bottom hole location on Green Canyon Block 202.
- Target reserves are in the Plio-Pleistocene sands at a depth of approximately 12,500 – 17,500 feet, subsea.

### DEVELOPMENT

- Shell announced in April 1999 its plans to develop Brutus utilizing a tension leg platform (TLP) to be installed on Green Canyon Block 158 in 2,985 feet of water.
- Total project cost is about \$800 MM, including pipelines, excluding lease costs. About 70 percent of the costs are associated with the fabrication and installation of the hull, deck, facilities, drilling rig and pipeline. The other 30 percent of the costs are related to drilling and completion of the wells.
- Batch setting of the eight wells was completed January 3, 2000 using Diamond's Ocean Worker semisubmersible drilling rig. Six of the planned development wells for the eight-slot TLP were subsequently predrilled to total depth following the batch set operations. Drilling operations using the Diamond Worker rig concluded in April 2001.

- An H&P contract platform rig completed all six pre-drilled wells and drilled and completed the two remaining wells.
- Installation of the TLP took place in June 2001. Heerema was the contractor for the installation using the derrick barge, Hermod.
- Oil production from the platform is transported approximately 26 miles via a 20-inch diameter pipeline to South Timbalier 301 "B" platform where it will be connected to the existing Amberjack System.
- Gas production from the platform is transported approximately 24 miles via a 20-inch gas pipeline and will be connected to the existing Manta Ray Offshore Gathering System in Ship Shoal Block 332.
- Average API gravity for the oil is low-mid 30 degrees. Oil/gas ratio is 70:30. Sulfur is 1.5%.

### **PRODUCTION**

- Production began in August 2001.
- The TLP facilities are designed to accommodate a peak gross production of approximately 100,000 barrels of oil per day and 150 million cubic feet of gas per day.

### **TLP ENGINEERING/CONSTRUCTION DETAILS**

- Design, engineering and project management for the Brutus TLP system was provided by Shell's Deepwater Services, with support from various design consultants.
- Completely assembled, the TLP is 3,250 feet high, from seafloor to the crown block of the drilling rig.
  - The TLP is designed to simultaneously withstand hurricane-force waves, currents and winds.
- Hull:
  - The hull is comprised of four circular steel columns, 66.5 feet in diameter and 166 feet high. pontoons, which connect the columns, are 35.5 feet wide and 23 feet high with a rectangular cross section.
  - The hull weighs approximately 13,500 tons, with a total displacement of 54,700 tons.
  - Daewoo Heavy Industries Co. of South Korea built the hull. On December 7, 2000, the hull left Daewoo's Okpo fabrication yard, transported by Dockwise's Mighty Servant 3. The hull arrived at CSO Gulf Maritime's integration facilities near Ingleside, TX on January 30, 2001.
- Deck:
  - The installed deck has dimensions at the outside truss rows of 245 feet square and approximately 40 feet high. The deck is composed of five modules: process, drilling, power, quarters, and wellbay.

- The deck modules are an open truss frame design with a total structural steel weight of approximately 7,650 tons.
- The total topside weight is approximately 22,000 tons, including all process equipment and the drilling rig.
- J. Ray McDermott built the modules at its Amelia, LA fabrication yard. The modules arrived at the CSO Gulf Marine integration yard in January and February 2001.

- Integration:

The hull and deck were integrated at the CSO Gulf Marine Ingleside fabrication yard near Corpus Christi, TX.

The five deck modules were lifted into position on the hull using the specialized lifting device originally developed for the Mars TLP integration.

- Tendons:

- There are 12 tendons, 3 per corner, each with a diameter of 32 inches and a wall thickness of 1.25 inches.
- Each tendon is approximately 2,900 feet long. The total weight for the 12 tendons is approximately 7,500 tons.
- The TLP foundation system is comprised of 12 piles, to which the tendons are attached.
- The piles are 82 inches in diameter and 340 feet long, weighing approximately 245 tons each.
- CSO Gulf Marine fabricated the piles and tendons at their Ingleside fabrication yard near Corpus Christi, TX.

- Drilling and Production Topsides:

- There are 8 well slots, with the well layout on the seafloor arranged in a rectangular pattern.
- The TLP supports a contract drilling rig, equipped with a surface BOP and high pressure drilling riser.
- There are complete separation, dehydration and treatment facilities designed to process 110,000 barrels of oil and condensate per day, plus 150 million cubic feet of gas per day and 30,000 barrels of produced water per day.
- The quarters module houses up to 94 people, and contains a control room and an emergency response center. In addition, temporary quarters modules are in place to allow for a maximum POB of 150 people during peak activity periods.

- Pipelines:

- A 20-inch diameter oil pipeline and 20-inch diameter natural gas pipeline will transport production.
- Installation of the steel catenary risers will occur immediately after TLP installation.
- J. Ray McDermott, Inc. installed the oil and gas pipelines beginning in the second quarter 2000 using the dynamically positioned Derrick Barge 16.

Subsea Tiebacks to Brutus:

- Production for two subsea tiebacks is processed at Brutus.
- The Glider prospect, operated by Shell (75%), has two producing wells that produce into Brutus for processing and sales. Glider is located in Green Canyon Block 248 and Newfield owns the remaining working interest.
- The J. Bellis prospect operated by LLOG (85%) with partner Davis (15%) in Green Canyon Block 157 has three wells that produce into Brutus for processing and sales.